AD-A097 624 INTERGRAPH CORP HUNTSVILLE AL F/G 12/1
HOMING MISSILE GUIDANCE STUDIES: OBSERVABILITY, ADAPTABILITY, A--ETC(U)
MAR 81 J L SPEYER, D G HULL DAAH01-80-D-0010
UNCLASSIFIED 81-016 NL

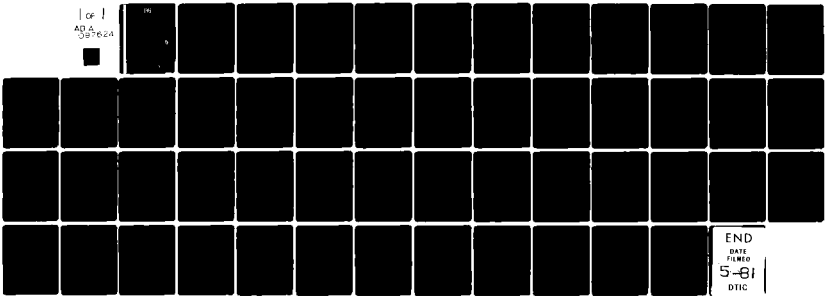

LEVEL II

(2)

81-016

AD A094234

HOMING MISSILE GUIDANCE STUDIES: OBSERVABILITY, ADAPTABILITY, AND THE LINEAR EXPONENTIAL GAUSSIAN GUIDANCE LAW

FINAL REPORT

March 31, 1981

Prepared for:

Guidance and Control Directorate
U. S. Army Missile Laboratory
U. S. Army Missile Command
Redstone Arsenal, Alabama 35898

INTERGRAPH CORPORATION

SECURITY CLASSIFICATION OF THIS PAGE (When Data Entered)

REPORT DOCUMENTATION PAGE		READ INSTRUCTIONS BEFORE COMPLETING FORM
1. REPORT NUMBER	2. GOVT ACCESSION NO. AD-A094 624	3. RECIPIENT'S CATALOG NUMBER
4. TITLE (and Subtitle) (16) Homing Missile Guidance Studies: Observability, Adaptability, and the Linear Exponential Gaussian Guidance Law		5. TYPE OF REPORT & PERIOD COVERED 9 Final Report,
		6. PERFORMING ORG. REPORT NUMBER 14 81-016
7. AUTHOR(s) (10) Dr. Jason L. Speyer, Dr. David G. Hull		8. CONTRACT OR GRANT NUMBER(s) (15) DAAH01-80-D-0010 Delivery Order No. 004
9. PERFORMING ORGANIZATION NAME AND ADDRESS Intergraph Corporation (formerly M&S Computing) One Madison Industrial Park, Huntsville, AL 35807		10. PROGRAM ELEMENT, PROJECT, TASK AREA & WORK UNIT NUMBERS (11) 31 Mar 81
11. CONTROLLING OFFICE NAME AND ADDRESS Commander U.S. Army Missile Command ATTN: DRSMI-RPT Redstone Arsenal, Alabama 35809		12. REPORT DATE March 31, 1981
		13. NUMBER OF PAGES 45 (12) 53
14. MONITORING AGENCY NAME & ADDRESS (if different from Controlling Office)		15. SECURITY CLASS. (of this report) UNCLASSIFIED
		15a. DECLASSIFICATION/DOWNGRADING SCHEDULE

16. DISTRIBUTION STATEMENT (of this Report)

Approved for public release, distribution unlimited.

17. DISTRIBUTION STATEMENT (of the abstract entered in Block 20, if different from Report)

18. SUPPLEMENTARY NOTES

19. KEY WORDS (Continue on reverse side if necessary and identify by block number)

Homing Missile Guidance
Gaussian Guidance Law
Kalman Filters
Extended Kalman Filter
LEG Guidance Law

20. ABSTRACT (Continue on reverse side if necessary and identify by block number)

The observability of system states is considered when angle information is available. The pseudolinear measurements are used to determine global observability for this nonlinear estimation problem. Also, the combination of the linear exponential Gaussian guidance law with an extended Kalman filter is considered.

DD FORM 1 JAN 73 1473 EDITION OF 1 NOV 65 IS OBSOLETE

SECURITY CLASSIFICATION OF THIS PAGE (When Data Entered)

PREFACE

This final report is a summary of the work performed by Intergraph Corporation (formerly M&S Computing, Inc.), for the Guidance and Control Directorate, U. S. Army Missile Laboratory, U. S. Army Missile Command, Redstone Arsenal, Alabama, under Contract No. DAAH01-80-D-0010, Delivery Order No. 004. Mr. Larry R. Murdock was the contract monitor for this effort, which was performed during the period June 11, 1980, to March 31, 1981.

Prepared by:

Dr. Jason L. Speyer, Consultant
Dr. David G. Hull, Consultant

Approved by:

Danny G. Jeffreys
Manager
System Evaluation

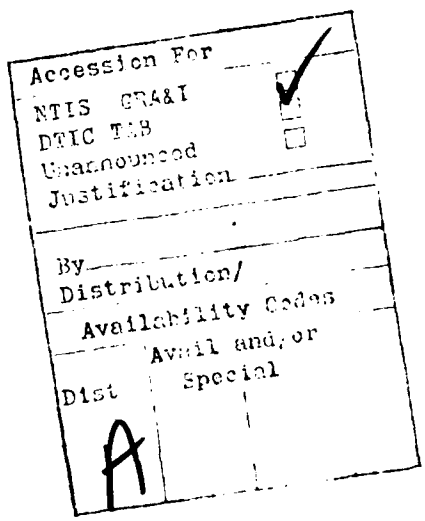

TABLE OF CONTENTS

LIST OF ILLUSTRATIONS

LIST OF ILLUSTRATIONS (Continued)

I. INTRODUCTION

This study is divided into two parts. First, the observability of the system states is considered when angle information is available. The pseudolinear measurements are used to determine global observability for this nonlinear estimation problem. An observer is constructed by defining a Lyapunov function of the estimation errors. Numerical experiments are used to determine the gains necessary to accurately determine all the states within the time of the engagement. If measurement noise is present, the filter is biased. Techniques of reducing the effect of the bias are explored. The second phase considers the combination of the linear exponential Gaussian (LEG) guidance law with an extended Kalman filter (EKF). The measurement variance of the EKF is estimated on-line. The error variance generated by the EKF is used in the LEG guidance law adaptively, changing its gains. This system is tested in a six-degree-of-freedom simulation of a bank-to-turn missile.

II. OBSERVABILITY OF THE MISSILE-TARGET ENGAGEMENT AND PSEUDOLINEAR MEASUREMENTS

The homing missile filtering problem is modeled with linear dynamics in a rectangular coordinate frame where the angle and relative range measurement functions are nonlinear. Our objective is first to investigate the observability of the engagement state space for this nonlinear system. It is demonstrated that if the missile acceleration is functionally different from that of the target acceleration, then all the states of the engagement are observable with angle information only. This is done by algebraic manipulation of the nonlinear measurement functions into a linear form called pseudo measurements. An observer is determined for these pseudo measurements, which guarantees that the estimation error will asymptotically converge to zero when the system is observable. A two-dimensional example of the homing engagement clearly shows that the states can be obtained perfectly from angle-only information. Earlier studies using pseudo measurements are discussed in References 1 and 2.[1,2] The present study is the first to investigate the use of pseudo measurements for the homing missile engagement.

The pseudo measurement system can be extended in the following ways. First, noise can be added to the original measurement functions. In three dimensions these measurements are composed of two angles, relative range, and relative range rate. The resulting pseudolinear measurements are linear with state-dependent noise. The particular form which has been chosen for the pseudo linear measurements is particularly useful when the range measurement is not available or has been substantially degraded. The observer structure that is developed could be used with the noisy measurements. However, a straightforward application of the observer produces biased estimates. This section concludes with a discussion of the extent of the biasing of the estimates and some possible directions for reducing these biases.

A. System Description

The missile engagement observation problem falls into a particular class of nonlinear observer problems which can be resolved using standard linear theory. In particular, the dynamic state is assumed linear as

$$x_{i+1} = A_i x_i + B_i u_i \qquad (1)$$

---

1. V. J. Aidala, "Behavior of the Kalman Filter Applied to Bearings - Only Target Motion Analysis," *Advances in Passive Tracking*, Vol. I, NPS-62TS 77001, Naval Postgraduate School, May, 1977.

2. A. G. Lindgren and K. F. Gong, "Position and Velocity Estimation via Bearing Observations," *IEEE Transactions on Aerospace and Electronic Systems*, Vol. AES-14, No. 4, July 1978.

where x_i is an n-dimensional state at time t_i, u_i is a p-dimensional control, and A_i and B_i are known matrices.

The measurement or observation function is

$$z_i = h_i(x_i) \tag{2}$$

where z_i is the q-dimensional observation and $h_i(x_i)$ is a known nonlinear q-dimensional function of the state x_i, where it is assumed that $q < n$. The particular classes of function of interest are those that can be algebraically manipulated into the form:

$$y_i(z_i) = H_i(z_i)x_i \tag{3}$$

where $y_i(z_i)$ is a known q-dimensional function of z_i, and $H_i(z_i)$ is a $q \times n$ known matrix of functions of z_i. The $y_i(z_i)$ are called psuedo measurements because they are derived from the original measurements z_i. Note that the desired form is a linear function of the states x_i. Conditions which guarantee that Equation (3) can be determined from Equation (2) are to be determined.

The objective is to design an observer for the linear dynamic system Equations (1) and (3). The important difference here is that $H(z_i)$ explicitly depends upon the original measurement. Since the control u_i affects z_i, the observability of the system equations (1) and (3), will depend upon the history of u_i as it affects $H(z_i)$. Nevertheless, the standard observability criterion,

$$W_{i,N} = \sum_{k=i}^{N} \Phi_{k,i}^T \, H_k^T(z_k) H_k(z_k) \Phi_{ki} > 0, \tag{4}$$

where

$$\Phi_{ki} = \prod_{j=i}^{k} A_j \, , \tag{5}$$

must hold along a trajectory for the states to be observable. That the standard Gramian holds for this class of observer problems is shown directly by producing the requirement of Equation (4) when attempting to determine the initial conditions. From Equation (3),

$$y_i(z_i) = H_i(z_i)x_i = H_i(z_i)\left[\Phi_{i0} \, x_0 + \sum_{j=1}^{i} \Phi_{ij} \, B_j \, u_j\right]. \tag{6}$$

Then, a sequence of psuedo measurements from 0 to k produces

$$\begin{bmatrix} Y_0(z_0) \\ \vdots \\ Y_k(z_k) \end{bmatrix} - \begin{bmatrix} 0 \\ \vdots \\ H_k(z_k) \sum_{j=0}^{k} \Phi_{kj} B_j u_j \end{bmatrix} = \begin{bmatrix} H_0(z_0) \\ \vdots \\ H_k(z_k)\Phi_{k0} \end{bmatrix} x_0 \qquad (7)$$

If Equation (7) is multiplied by $[H_0(z_0),.....,\Phi_{k0}^T H_k^T(Z_k)]$, then the requirement that x_0 be determined is that $W_{k,0}$ be invertable. Note that if x_0 is observable, it can be determined in a finite time.

B. Observers with Pseudolinear Measurements

Since the dynamic system equations (1) and (3) are linear, a linear observer structure is chosen. The gain for the observer is chosen to guarantee that a function $V(e_i)$ be a Lyapunov function, where e_i is the error in the estimate of the state. The observer structure is chosen as

$$\hat{x}_{i/i} = x_{i/i-1} + K_i(y_i(z_i) - H_i(z_i)\hat{x}_{i/i-1}) \qquad (8)$$

$$x_{i+1/i} = A_i \hat{x}_{i/i} + B_i u_i \qquad (9)$$

where $x_{i/i}$ is the estimate of the state processing all the information up to time stage i, $x_{i/i-1}$ is the estimate of the state processing all the information up to time stage i - 1, and K_i is the observer gain to be determined by ensuring that the function $V(e_i)$ be a Lyapunov function. An interesting feature of this observer is that it is a nonlinear function of the measurements.

First, the propagation for the error is determined. Define the errors e_i and $\bar{e}_i$, respectively, as

$$e_i \triangleq x_i - \hat{x}_{i/i}, \quad \bar{e}_i \triangleq x_i - \hat{x}_{i/i-1}. \qquad (10)$$

Then from Equations (8) and (9), the propagation equations for the errors are

$$e_i = (I - K_i H_i)\bar{e}_i \qquad (11)$$

$$\bar{e}_{i+1} = A_i e_i. \qquad (12)$$

Define a Lyapunov function as

$$V_i = e_i^T P_i^{-1} e_i > 0, \qquad (13)$$

where P_i is a positive definite matrix. For convenience, a second quadratic function is defined as

$$\bar{V}_i = \bar{e}_i^T M_i^{-1} \bar{e}_i > 0 \tag{14}$$

where M_i is a positive definition matrix.

For the error to be asymptotically stable, it is required that

$$V_{i+1} - \bar{V}_{i+1} \leq 0 \tag{15}$$

$$\bar{V}_{i+1} - V_i < 0. \tag{16}$$

This implies that $V_{i+1} - V_i < 0$ and, therefore, is a monotonically decreasing function. The derivation begins with Equation (15), which is expanded using Equation (11) as

$$V_i - \bar{V}_i = \bar{e}_i^T [(I - K_i H_i)^T P_i^{-1} (I - K_i H_i) - M_i^{-1}] \bar{e}_i \leq 0. \tag{17}$$

A sufficient condition for the inequality in Equation (17) to hold is that the matrix in Equation (17) is nonpositive definite. This is ensured by

$$(I - K_i H_i)^T P_i^{-1} (I - K_i H_i) - M_i^{-1} = -H_i^T (H_i M_i H_i^T + R_i)^{-1} H \tag{18}$$

where R_i is a qxq positive definite matrix. Since $H_i M_i H_i^T + R_i$ is the sum of the two positive definite matrices, the inverse exists, and the right side of Equation (18) is nonpositive definite. The choices of matrices anticipate the construction of observer gains that resemble the formulism used in constructing gains for the Kalman filter. For example, R_i plays a role similar to that of the measurement noise variance in the Kalman filter formulation. Rewrite Equation (18) as

$$\begin{aligned}(I - K_i H_i)^T P_i^{-1} (I - K_i H_i) &= M_i^{-1} - H_i^T \left(H_i M_i H_i^T + R_i\right)^{-1} H_i \\ &= M_i^{-1} \left[M_i - M_i H_i^T \left(H_i M_i H_i^T + R_i\right)^{-1} H_i M_i \right] M_i^{-1}\end{aligned} \tag{19}$$

where the second equality results from a standard matrix identity. By taking the inverse of both sides, Equation (19) becomes

$$P_i = (I - K_i H_i) M_i \left[M_i - M_i H_i^T \left(H_i M_i H_i^T + R_i\right)^{-1} H_i M_i \right]^{-1} M_i (I - K_i H_i)^T . \tag{20}$$

If the observer gain is chosen as

$$K_i = M_i H_i^T \left(H_i M_i H_i^T + R_i\right)^{-1}, \tag{21}$$

then Equation (20) reduces to

$$P_i = M_i - M_i H_i^T (H_i M_i H_i^T + R_i)^{-1} H_i M_i$$

$$= (M_i^{-1} + H_i^T R_i H_i)^{-1} \tag{22}$$

where the last line is obtained using a standard matrix identity. For M_i and R_i positive definite, the last line clearly shows that P_i is positive definite. Equation (22) is essentially the update formula in the Kalman filter.

To determine M_i, Equation (16) is used with Equation (12) as

$$V_{i+1} - V_i = e_i^T (A_i^T M_{i+1} A_i - P_i^{-1}) e_i < 0. \tag{23}$$

A sufficient condition for the inequality of Equation (23) to hold is if the matrix of Equation (23) is negative definite. This is ensured by choosing

$$A_i^T M_{i+1}^{-1} A_i - P_i^{-1} = -P_i^{-1} A_i^{-1} (Q_i^{-1} + A_i^{-T} P_i^{-1} A_i^{-1})^{-1} A_i^{-T} P_i^{-1} \tag{24}$$

where Q_i is non-negative definite and A_i is assumed invertable. (This is always the case if A_i is a transition matrix obtained from a linear dynamic system.) Since P_i is positive definite, then the right side of Equation (24) must also be positive definite. The particular form chosen was needed to simplify Equation (24) using the matrix identify given in Equation (22); that is,

$$M_{i+1}^{-1} = A_i^{-T} P_i^{-1} A_i^{-1} - A_i^{-T} P_i^{-1} A_i^{-1} (Q_i^{-1} + A_i^{-T} P_i^{-1} A_i^{-1})^{-1} A_i^{-T} P_i^{-1} A_i^{-1}$$

$$= (A_i P_i A_i^T + Q_i)^{-1} \tag{25}$$

or

$$M_{i+1} = A_i P_i A_i^T + Q_i. \tag{26}$$

This is the propagation equation used in the Kalman filter. Therefore, starting with a positive definite P_0, Equations (22) and (26) propagate a positive definite P_i. Then, the observer gain can be calculated from Equation (21).

If the system equations (1) and (3) are observable, then P_i will be bounded. Therefore, since the Lyapunov function $V(e_i)$ is constantly decreasing for all finite i and since P_i^{-1} must be bounded from below, then $e_i \to 0$ as $i \to \infty$.

C. Dynamic Description of Homing Missile Problem

The system dynamics of the missile intercept problem written in rectangular coordinates and the associated measurement process is a particular example of the system described in subsection IIA. The state vector x is a nine-state vector composed of three relative positions $X_R^T \triangleq [X, Y, Z]$, three relative velocities $v_R^T = [v_X, v_Y, v_Z]$, and three target accelerations $a_T^T \triangleq (a_X, a_Y, a_Z)$. The continuous dynamic system is

$$\dot{x} = Fx + Gu \tag{27}$$

where u is the missile acceleration, used here as the control vector, and where it is assumed that the autopilot is sufficiently fast to produce negligible error. The dynamic coefficients for Equation (27) are*

$$F = \begin{bmatrix} 0 & I_3 & 0 \\ 0 & 0 & I_3 \\ 0 & 0 & -\lambda I_3 \end{bmatrix} \quad , \quad G = \begin{bmatrix} 0 \\ -I_3 \\ 0 \end{bmatrix} \tag{28}$$

where λ is the average target switch time when approximating a Poisson process. This system can be put in the discrete form of Equation (1) where

$$A_i = \begin{bmatrix} I_3 & I_3\,\Delta t & I_3\left(\frac{1}{\lambda^2}\,e^{-\lambda\Delta t} + \lambda\Delta t - 1\right) \\ 0 & I_3 & I_3\left(\frac{1}{\lambda} - \frac{1}{\lambda}e^{-\lambda\Delta t}\right) \\ 0 & 0 & I_3 e^{-\lambda\Delta t} \end{bmatrix} \tag{29}$$

$$B_i = \begin{bmatrix} -I_3(\Delta t)^2/2 \\ I_3\,\Delta t \\ 0 \end{bmatrix} \tag{30}$$

where Δt is the sample time in the discretization of the continuous dynamic system.

The intercept geometry and measurement angles and relative range are given in Figure 1. The azimuth and elevation angle measurements are

$$az = \tan^{-1}(Y/X) \tag{31}$$

$$el = \tan^{-1}[-Z/(X^2 + Y^2)^{1/2}] \tag{32}$$

and the relative range and range rate measurements are

$$R = \sqrt{X^2 + Y^2 + Z^2} \tag{33}$$

*I_n is an $n \times n$ identity matrix.

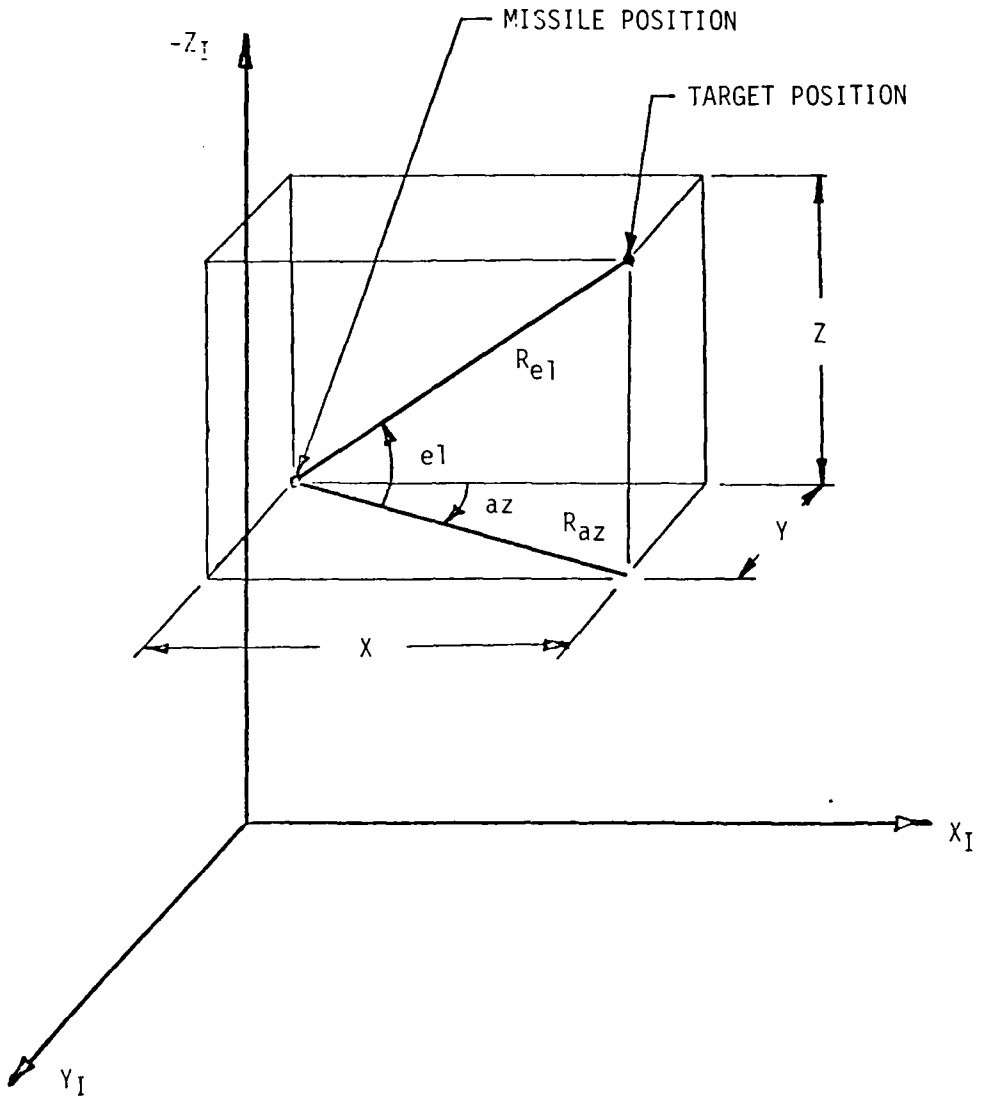

Figure 1. Intercept geometry and measurement angles.

$$\dot{R}_R = (Xv_X + Yv_Y + Zv_Z)/R_R. \quad (34)$$

D. Transformation of Original Nonlinear Measurements Into Pseudolinear Measurements

The three measurements are transformed into pseudolinear measurements by straightforward use of trigonometric identities. The results obtained here can be extended to the case where these measurements are corrupted by additive white noise. From Equation (31), the pseudo measurement is

$$y_1 = 0 = X \sin az - Y \cos az. \quad (35)$$

The pseudo measurement y_1 is always zero. Before proceeding to the elevation angle measurement, note that

$$\sqrt{X^2 + Y^2} = X \cos az + Y \sin az. \quad (36)$$

Then, from Equation (32),

$$y_2 = 0 = (X^2 + Y^2)^{1/2} \sin el + z \cos el. \quad (37)$$

With Equation (36), Equation (37) reduces to

$$y_2 = 0 - X \cos az \sin el + Y \sin az \sin el + Z \cos el. \quad (38)$$

Again, the pseudo measurement is always zero. Note that this formulation of pseudo measurements does not depend upon the range measurement and, therefore, can be used in studies where only angle measurements are available or the range measurement is very degraded.

For the range measurement, an identity similar to Equation (35) can be constructed as

$$y_3 = R_R = -Z \sin el + (X^2 + Y^2)^{1/2} \cos el. \quad (39)$$

But from Equation (36), it is seen that

$$y_3 = R_R = X \cos az \cos el + Y \sin az \cos el - Z \sin el. \quad (40)$$

In this case, R_R remains the measurement, but it is now expanded as a linear function of the states. Similarly, the range-rate measurement can be converted into a pseudolinear form as

$$y_3 = \dot{R}_R = \frac{Xv_X}{R_R} + \frac{Yv_Y}{R_R} - v_Z \sin el$$

$$= v_X \cos el \cos az + v_Y \cos el / \sin az - v_z \sin el. \quad (41)$$

In this way, all the usual measurements which are nonlinear in a cartesian reference frame are converted to a linear form. However, the coefficient matrix is a nonlinear function of the original measurements.

E. Observability of the State Space Using Pseudolinear Measurements

Conditions for the observability of the dynamic state are now investigated. To simplify this study, the dynamic model is reduced to a plane. Our objective is to show that, if the missile acceleration is functionally different from that of the target, the full dynamic state is observable. Conditions for observability are discussed using constant target acceleration. In this section the planar homing problem is presented using the observer developed in subsection IIB.

Consider a simple dynamic system as

$$\dot{X} = V_X,\ \dot{Y} = v_Y,\ \dot{v}_X = a_X - u_X,\ \dot{v}_Y = a_Y - u_Y,\ \dot{a}_X = 0,$$
$$\dot{a}_Y = 0 \tag{42}$$

where u_X and u_Y are the missile accelerations and a_X and a_Y are the target accelerations. Suppose further that a_X and a_Y are modeled as constants as indicated in Equation (42). The goal is to determine the initial states from a sequence of angle-only measurements given by the pseudolinear measurement of Equation (35). The result is the following:

$$\begin{bmatrix} \sin az_1 & -\cos az_1 & t_1 \sin az_1 & -t_1 \cos az_1 & t_{1/2}^2 \sin az_1 & -t_{1/2}^2 \cos az_1 \\ \sin az_2 & -\cos az_2 & t_2 \sin az_2 & -t_2 \cos az_2 & t_{2/2}^2 \sin az_2 & -t_{2/2}^2 \cos az_2 \\ \sin az_3 & -\cos az_3 & t_3 \sin az_3 & -t_3 \cos az_3 & t_{3/2}^2 \sin az_3 & -t_{3/2}^2 \cos az_3 \\ \sin az_4 & -\cos az_4 & t_4 \sin az_4 & -t_4 \cos az_4 & t_{4/2}^2 \sin az_4 & -t_{4/2}^2 \cos az_4 \\ \sin az_5 & -\cos az_5 & t_5 \sin az_5 & -t_5 \cos az_5 & t_{5/2}^2 \sin az_5 & -t_{5/2}^2 \cos az_5 \\ \sin az_6 & -\cos az_6 & t_6 \sin az_6 & -t_6 \cos az_6 & t_{6/2}^2 \sin az_6 & -t_{6/2}^2 \cos az_6 \end{bmatrix} \begin{bmatrix} X(0) \\ Y(0) \\ v_X(0) \\ v_Y(0) \\ a_X(0) \\ a_Y(0) \end{bmatrix}$$
$$= \begin{bmatrix} X_m(t_1) \sin az_1 - Y_m(t_1) \cos az_1 \\ X_m(t_2) \sin az_2 - Y_m(t_2) \cos az_2 \\ X_m(t_3) \sin az_3 - Y_m(t_3) \cos az_3 \\ X_m(t_4) \sin az_4 - Y_m(t_4) \cos az_4 \\ X_m(t_5) \sin az_5 - Y_m(t_5) \cos az_5 \end{bmatrix} \tag{43}$$

where a numerical subscript denotes time and

$$X_m(t) \triangleq \int_0^t \int_0^\sigma u_X(\tau)\, d\tau\, d\sigma,\ Y_m(t) \triangleq \int_0^t \int_0^\sigma u_Y(\tau)\, d\tau\, d\sigma\ . \tag{44}$$

If the missile acceleration is zero, then the right side of Equation (43) becomes zero. Therefore, the rank of the cooefficient matrix must be less than six. Observability is reduced to determining the eigenvectors associated with the zero eigenvalues of the coefficient matrix. If $d(az)/dt \neq 0$, then the rank of the coefficient matrix is five, and there is

only one eigenvector direction. Therefore, the direction of the initial condition is observable but not the magnitude. If d(az)/dt = 0, then there are numerous directions so that even the direction is not uniquely determined.

If the missile acceleration is a constant, then the right side of Equation (43) is nonzero. However, there is no way to determine the difference between the unknown constant target acceleration and the missile acceleration. Therefore, the coefficient matrix must still have rank less than six and be singular. In this case, the signatures generated by the missile and target accelerations are the same and cannot be distinguished.

If the missile acceleration is not a constant, i.e., the missile acceleration is nonzero but with a different time function than the target acceleration, then the coefficient matrix becomes invertable, and the initial state is observable from the angle-only measurement. In the next section the observer developed in subsection IIB is applied to the homing missile problem described in subsection IIC, but in the plane. The results demonstrate quite clearly the observability of the state for the homing problem with angle information only.

F. Application of Pseudolinear Observer to the Homing Missile Engagement

The observer developed in subsection IIB is applied to the homing missile guidance planar problem. The dynamics used in the simulation for testing the observer and determining its response are exactly the same as those assumed in the observer. In this way the performance of the observer can be studied without the corrupting effects of unmodeled complex nonlinearities.

The homing missile guidance scheme is derived by using linear-quadratic theory.[3] The guidance law is of the form

$$u = \Lambda_1(\hat{\tau}_g)X_R + \Lambda_2(\hat{\tau}_g)\hat{v}_R + \Lambda_3(\hat{\tau}_g)\hat{a}_T \tag{45}$$

where the guidance gains based on estimated time-to-go, τ_g, are

$$\Lambda_1(\tau_g) = I_2\, N(\tau_g)/\tau_g^2 \tag{46}$$

$$\Lambda_2(\tau_g) = I_2\, N(\tau_g)/\tau_g \tag{47}$$

$$\Lambda_3(\tau_g) = I_2\, N(\tau_g)\,(e^{-\lambda\tau_g} + \lambda\tau_{g-1})/(\lambda^2\,\tau_g^2) \tag{48}$$

where estimated time-to-go is calculated as

$$\hat{\tau}_g \Lambda -|X_R|^2/(\hat{v}_R \cdot \hat{X}_R) \tag{49}$$

3. A. E. Bayson and Y.-C. Ho, *Applied Optimal Control*, Blaisdell, Waltham, Massachusetts, 1969.

where X_R, v_R and a_T are the estimated states from the observer, and the navigation ratio is

$$N(\tau_g) = 3\tau_g^3/(3\gamma + \tau_g^3). \tag{50}$$

The value of γ is chosen as 0.0001.

The observer derived in subsection IIB is evaluated for the homing planar problem using only the pseudolinear measurement [Equation (35)]. The responses are chosen by picking various values of P_0, Q, and R. In the stochastic counterpart, these parameters, when used in the Kalman filter, play the role of the initial error variance, the process noise variance, and the measurement noise variance, respectively. However, if white noise is actually added to the measurement, the estimate will be biased. As discussed in subsection IIG, the observer used as a filter must be modified. Nevertheless, it is anticipated that if the noise is small enough, the bias effects will also be small. Therefore, values of R, Q, and P_0 are chosen over a range of values that would be used in a statistical setting.

The observer derived in subsection IIB is initialized by the following data.

The actual initial states are:

$X = 7000$ ft, $Y = 100$ ft, $v_X = -1000$ ft/sec, $v_Y = -100$ ft/sec,

$a_X = 10$ ft/sec^2, $a_Y = 10$ ft/sec^2.

The initial estimate states are

$\hat{X} = 5500$ ft, $\hat{Y} = 0$ ft, $\hat{v}_X = -800$ ft/sec, $\hat{v}_Y = 0$ ft/sec

$\hat{a}_X = 0$ ft/sec^2, $\hat{a}_Y = 0$ ft/sec^2 .

The initial value of P is always diagonal. The six diagonal elements are $P_{11} = 10^4$, $P_{22} = 10^4$, $P_{33} = 10^4$, $P_{44} = 10^4$, $P_{55} = 10^2$, and $P_{66} = 10^2$ unless otherwise specified.

The value of Q is always chosen as zero and $\lambda = 1$. With the above values, the responses of the observer for values of $R = (0, 10^{-8}, 10^{-6}, 10^{-4}, 10^{-2})$ are shown in Figures 2 through 7. Clearly, the speed of the response is related to the value of R. Large overshoots in acceleration occur for the low values of R which produce a high gain system. In Figures 8 through 10, the observer response to various values of initial P with $R = 10^{-6}$ and $Q = 0$ are shown. Only the responses in the X direction are shown since variations in the Y direction are not very different from those shown in Figures 3, 5, and 7. The effect of various values of $P_{55} = P_{66}$ on the position response is not great until $P_{55} = P_{66} = 10^5$. The most significant effect is in the large acceleration errors that occur early in the response as shown in Figure 10. Effects of variation in Q have been computed,

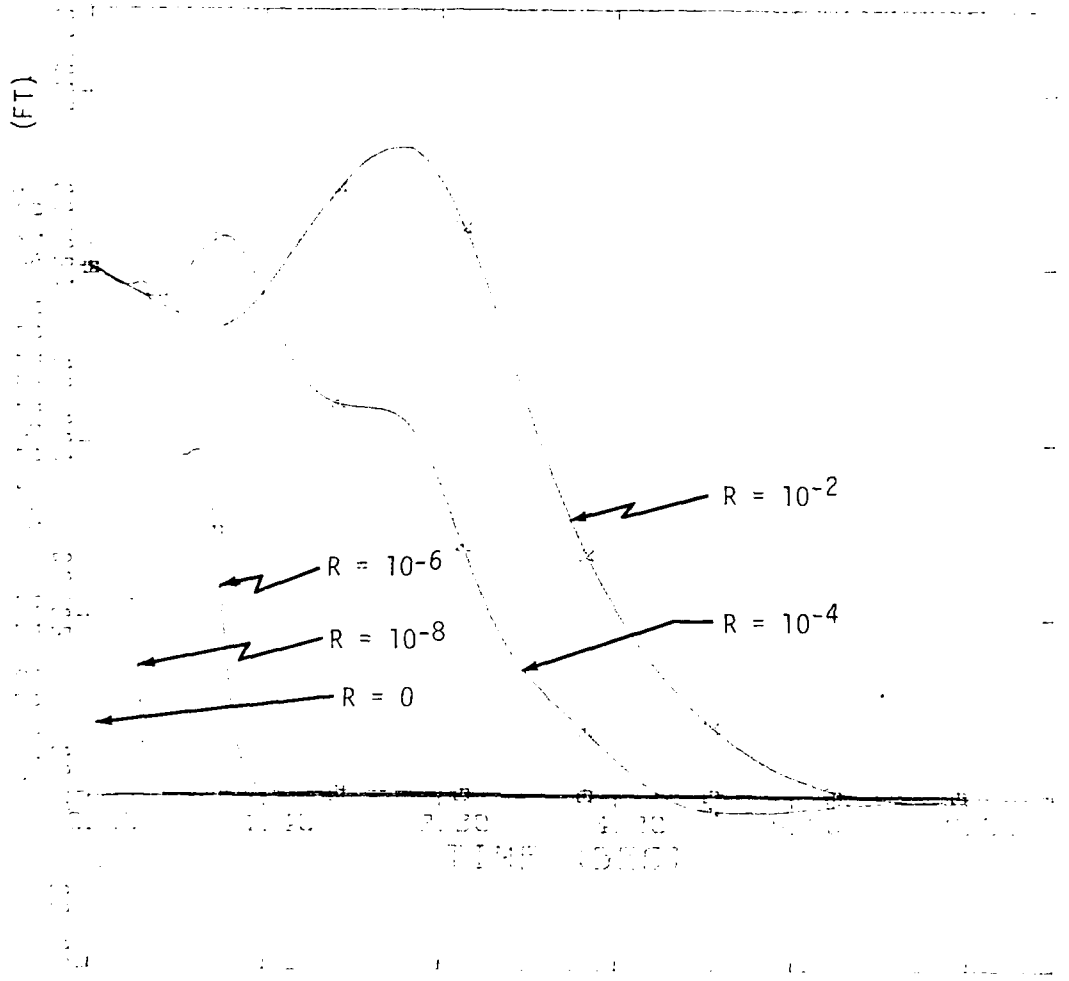

Figure 2. Error history in X-position for various values of R (angle-only measurement).

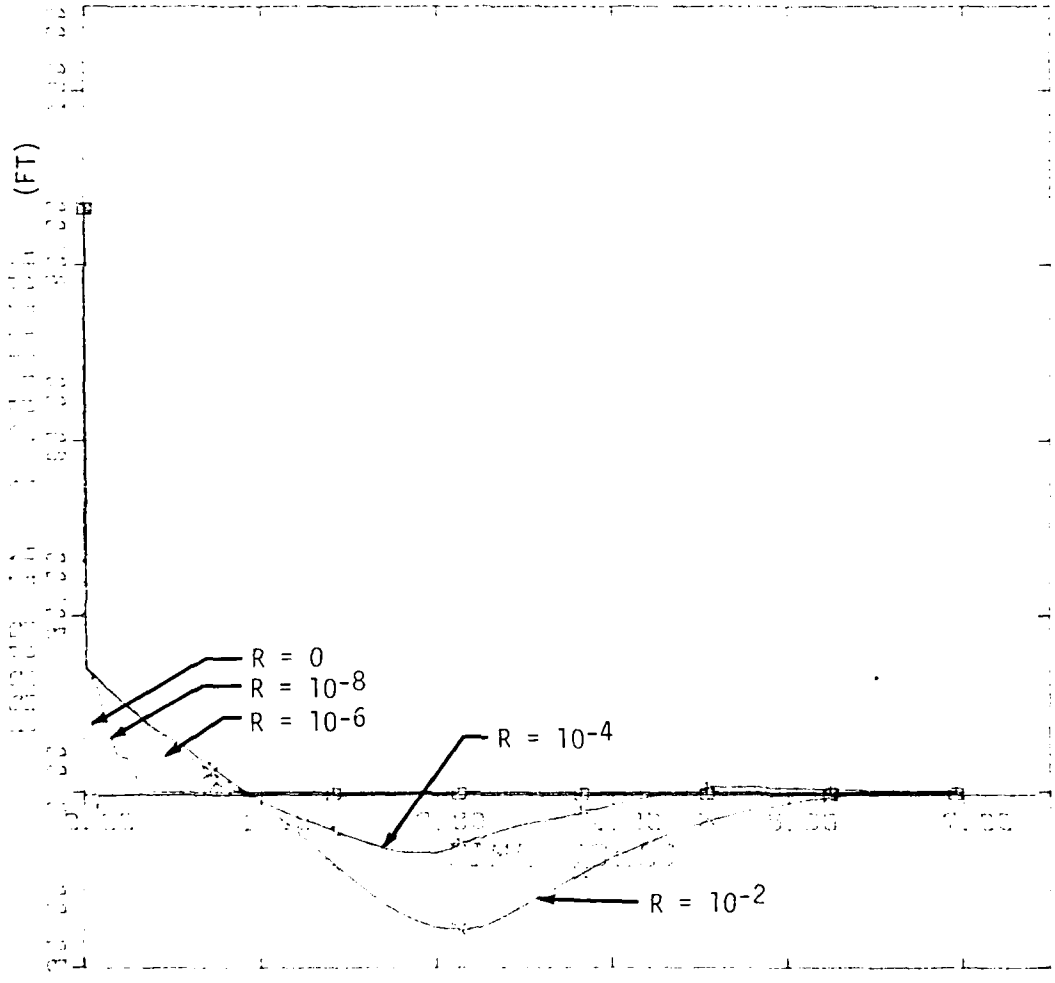

Figure 3. Error history in Y-position for various values of R (angle-only measurement).

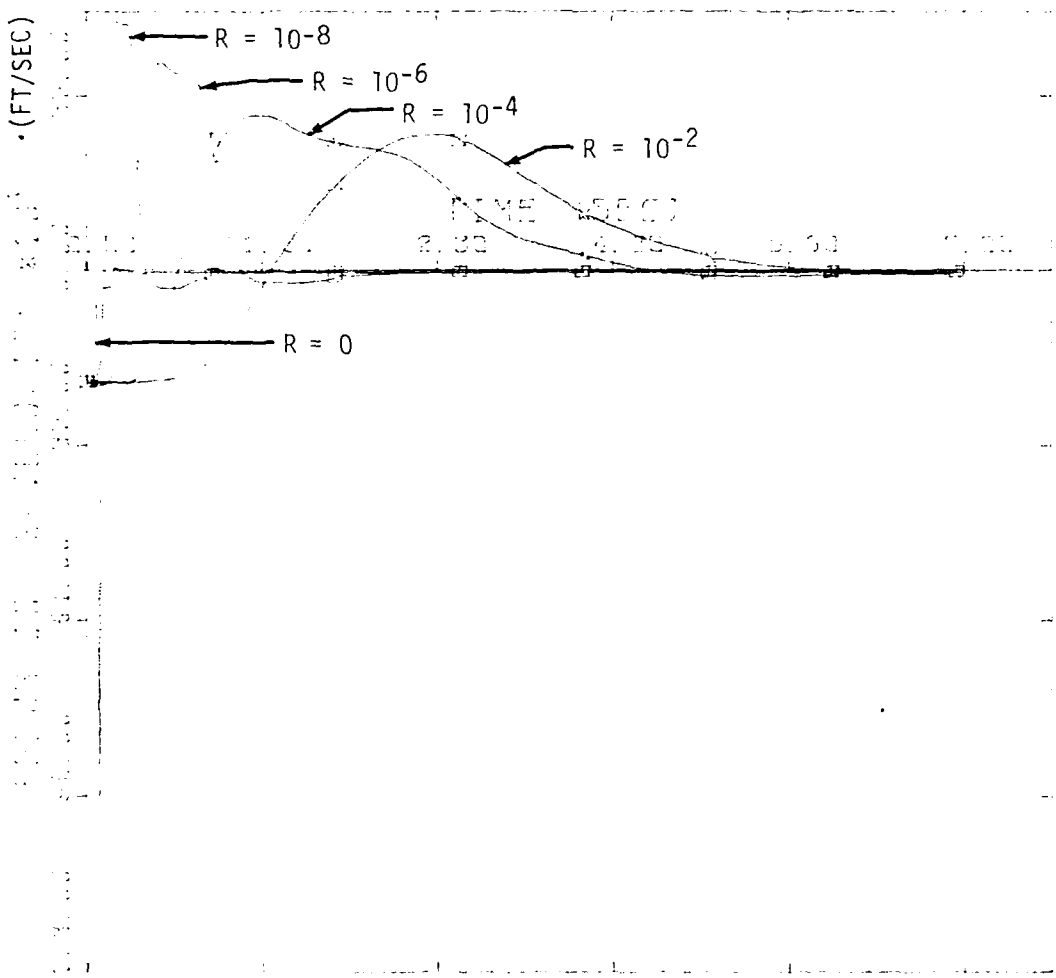

Figure 4. Error history in X-velocity for various values of R (angle-only measurement).

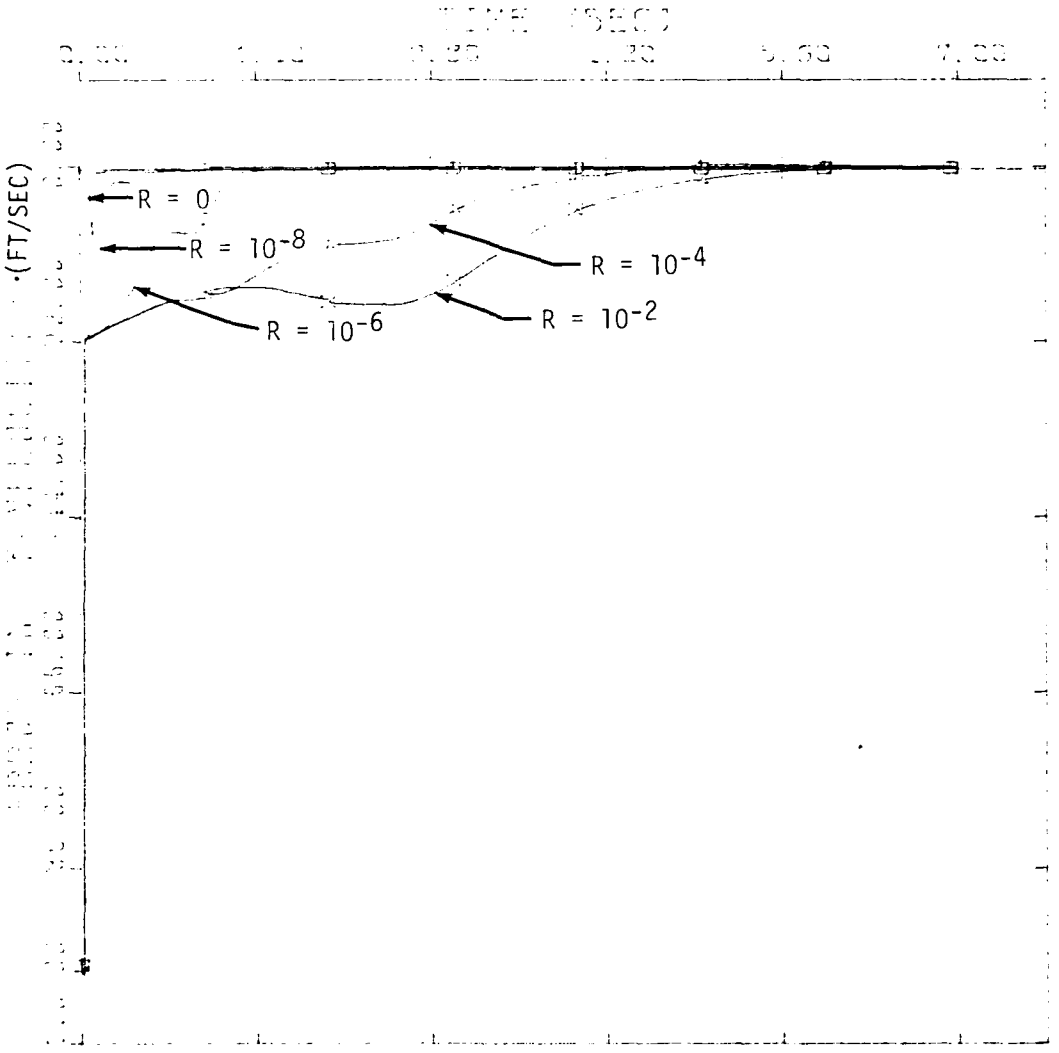

Figure 5. Error history in Y-velocity for various values of R (angle-only measurement).

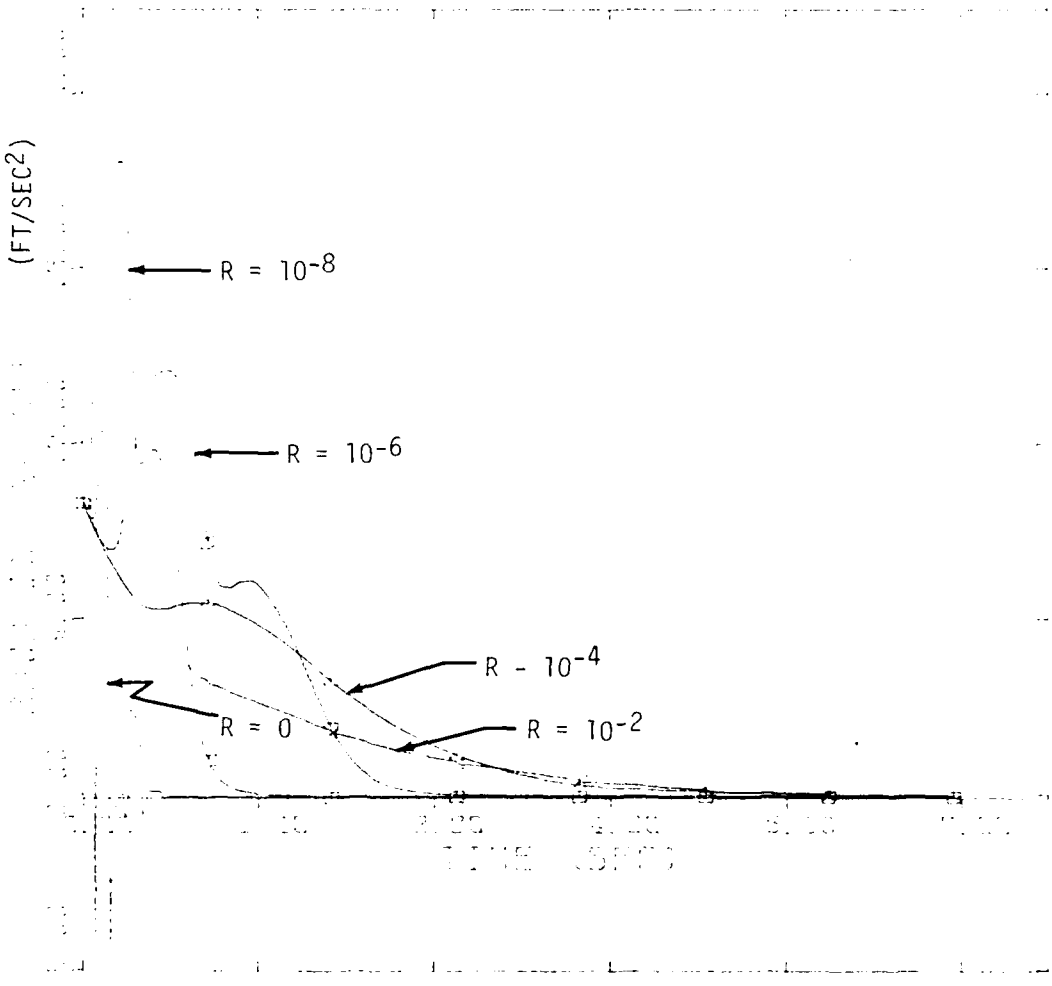

Figure 6. Error history in X-acceleration for various values of R (angle-only measurement).

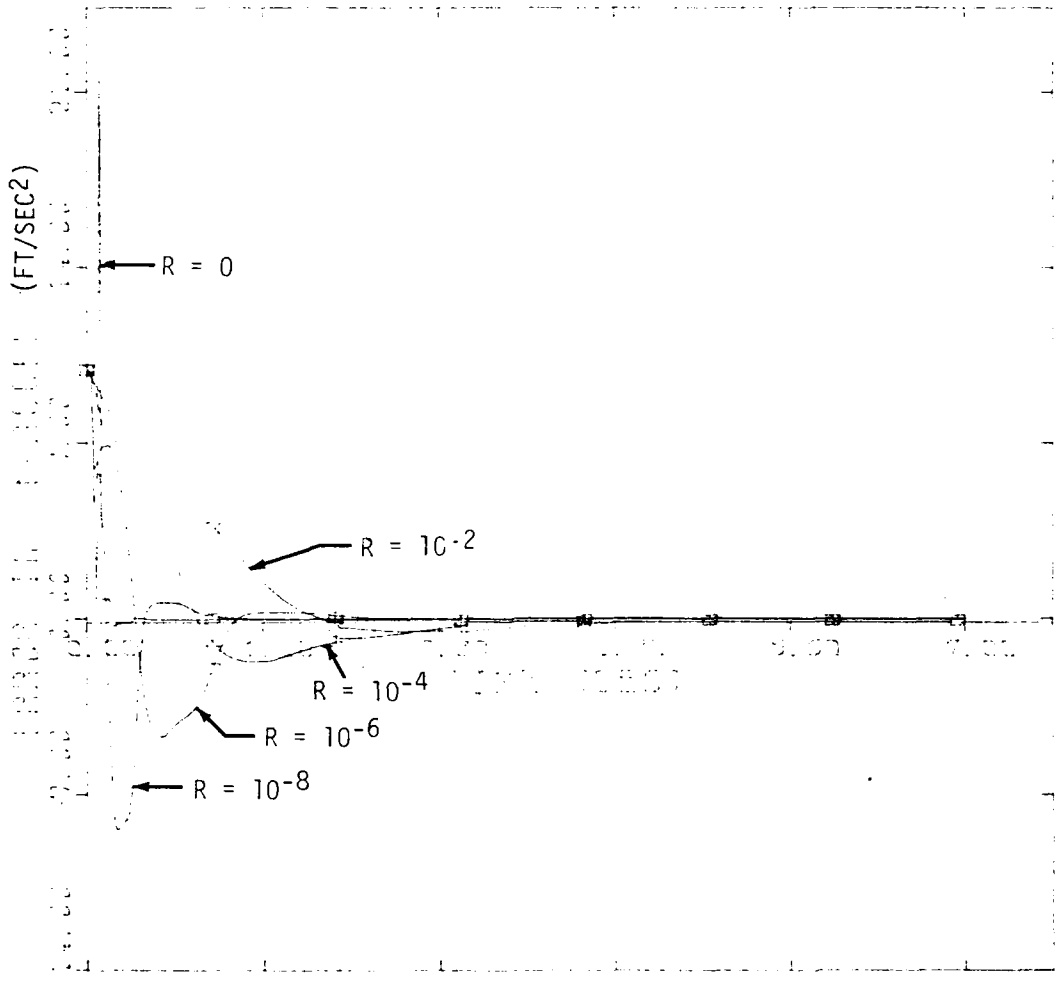

Figure 7. Error history in Y-acceleration for various values of R (angle-only measurement).

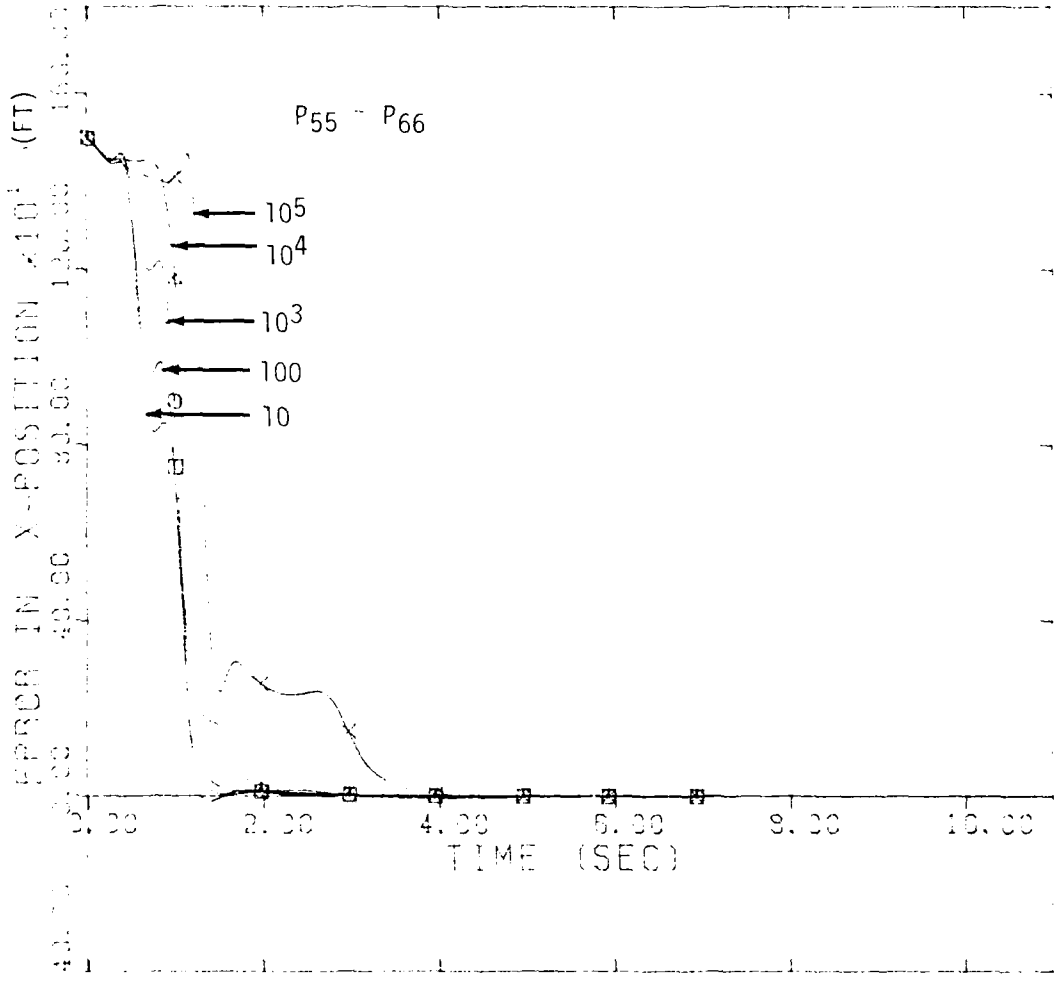

Figure 8. Error history in X-position for various values of $P_{55} = P_{66}$ (angle-only measurement).

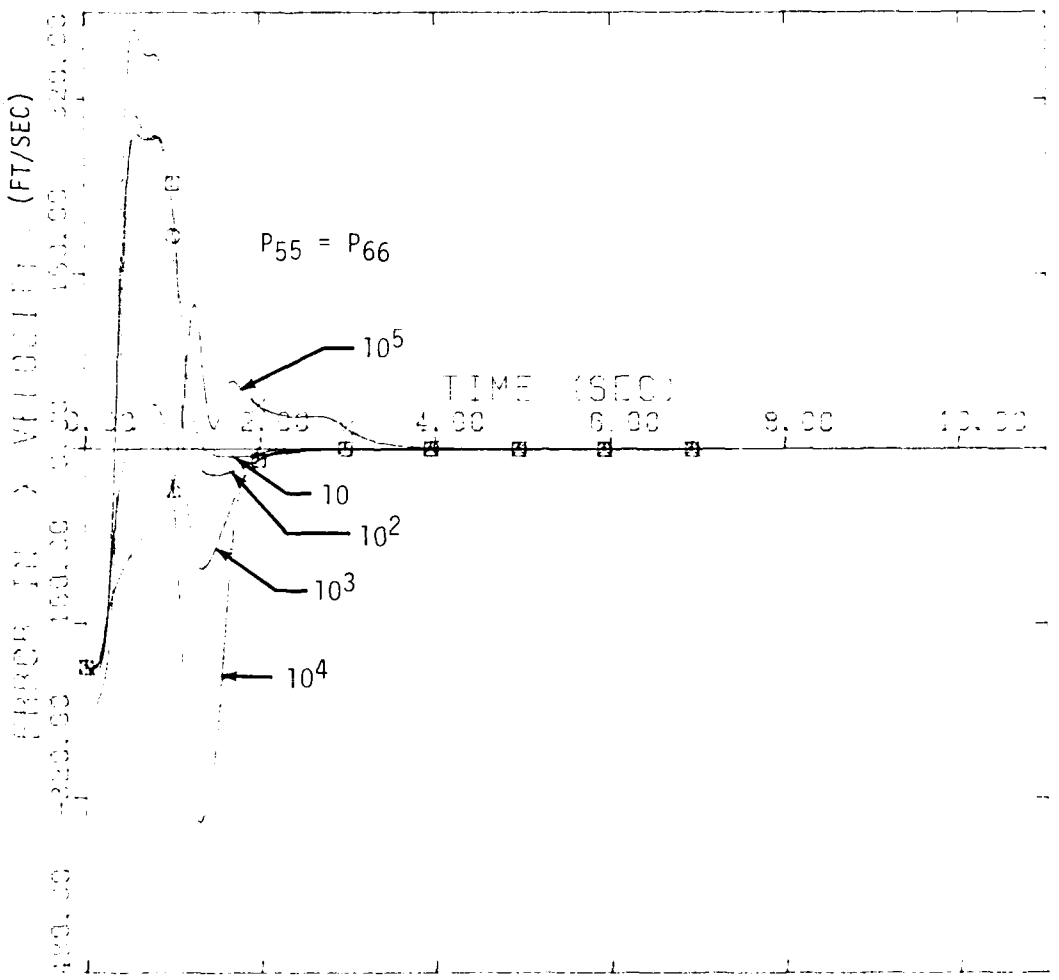

Figure 9. Error history in X-velocity for various values of $P_{55} = P_{66}$ (angle-only measurement).

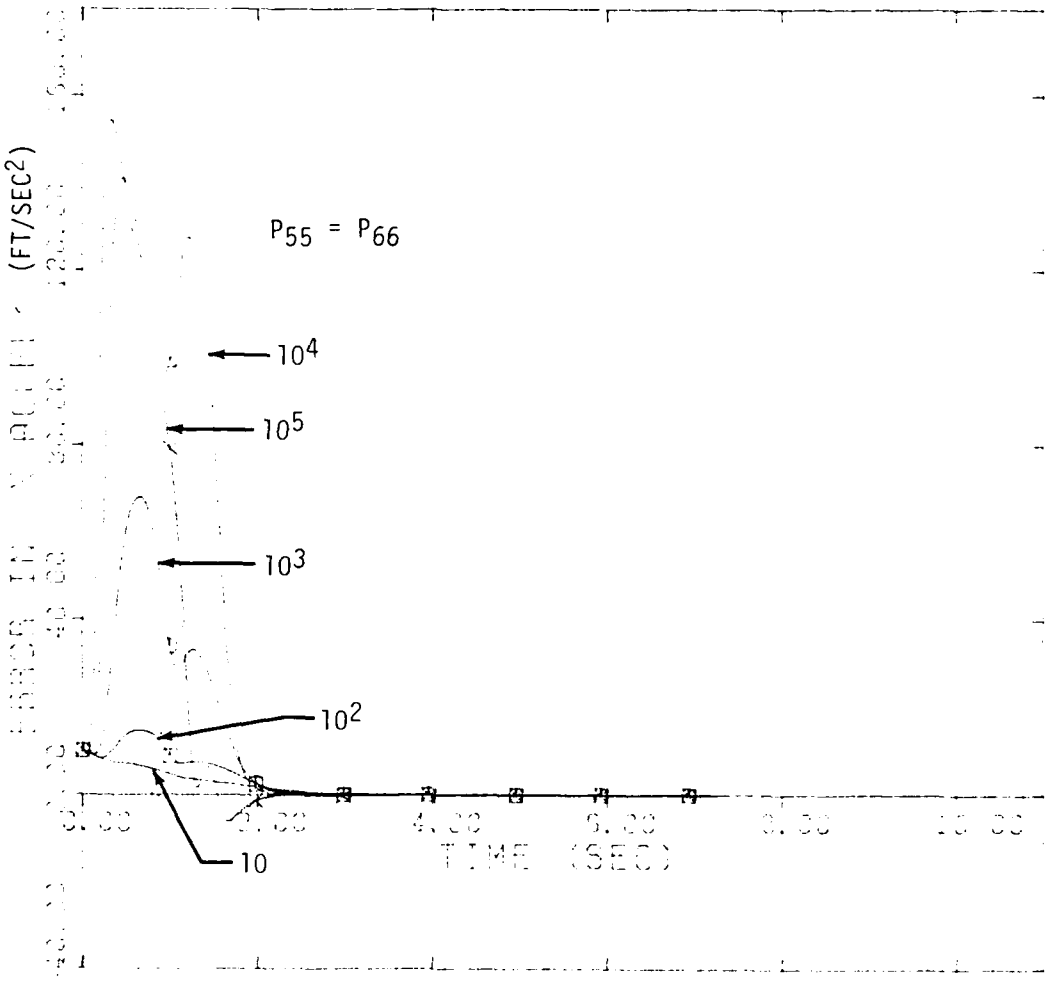

Figure 10. Error history in X-acceleration for various values of $P_{55} = P_{66}$ (angle-only measurement).

but the results have not been explained. The above data is preliminary and a continuing effort should be made in understanding the performance of this observer. For example, the performance of the pseudomeasurement observer should be compared with an observer constructed as an extended Kalman filter. The performance of these observers operating without noise should form a lower bound on the performance of similar observers operating in a noisy environment. Furthermore, the region of validity of the linearization of the extended Kalman can be assessed.

G. Effect of Noise on the Estimates of the Observer Using Pseudolinear Measurements

If the measurements are corrupted by noise, then the measurements of Equations (31) to (34) are rewritten as

$$az_m = az + v_1,\ el_m = el + v_2,\ R_m = R_R + v_3,$$
$$\dot{R}_m = \dot{R}_R + v_4 \tag{51}$$

where v_1 through v_4 are white Gaussian noise processes. The Gaussian assumption can be relaxed if only linear filter structures are considered. Again, these measurements can be converted into pseudolinear measurements. For example, the pseudolinear measurement for azimuth angle is

$$y_1 = 0 = \sin az_m\, x - \cos az_m\, Y - (X^2 + Y^2)^{1/2} \sin v_1. \tag{52}$$

Similar results can be obtained for the other three measurements.

In general, the measurement function [Equation (2)] with additive noise becomes

$$z_i = h_i(x_i) + v_i \tag{53}$$

where v_i is a vector of white noise. The pseudo measurements are assumed to take the form

$$y_i(z_i) = H_i(z_i)x_i + \nu_i(x_i, v_i) \tag{54}$$

where $\nu_i(x_i, v_i)$ is a state-dependent white noise process. The pseudo measurement of Equation (52) is an example of Equation (54).

In this section, the effect of the noise process $\nu_i(x_i, v_i)$ on the estimates produced by the observer of subsection IIB when used as a filter is determined. It is shown that these estimates are biased. Directions in constructing filters which reduce this bias are discussed. As has been assumed for the observer, a linear structure is assumed for the filter as

$$\hat{x}_i = L_i\, x_i + K_i\, y_i. \tag{55}$$

The gains L_i and K_i are to be chosen so that the estimates are unbiased. In attempting to do this, the error in the estimate is formed using Equation (10) as

$$e_i = (I - K_i H_i(z_i) - L_i)x_i + L_i \bar{e}_i - K_i \nu_i (x_i, v_i) . \quad (56)$$

Suppose the gains are chosen so that the coefficient of x_i is made zero. Then the gains L_i and K_i would become functions of the present measurement z_i as

$$L_i(z_i) = I - K_i(z_i) H_i(z_i), \quad (57)$$

which results in the structure assumed for the observer of subsection IIB.

If the estimates are unbiased, then the unconditional expectation of the error is zero. If the unconditional expectation of Equation (56) is taken using Equation (57), then both $\bar{e}_i$ is correlated with $L_i(z_i)$ and $\nu_i(x_i, v_i)$ is correlated with $K_i(z_i)$. To separate the gains from the state, error, and measurement noise, the conditional expectation is first taken. Because of the nesting property of conditional expectation, the unconditional expectation can be taken over the conditional mean. If the conditional mean is zero, then the conditional mean will be zero. Therefore, the conditional expectation of Equation (56) with respect to the measurement history $Z_i \triangleq \{z_1, \ldots . z_i\}$ is

$$E\{e_i/Z_i\} = L_i(z_i) E\{\bar{e}_i/Z_i\} - K_i(z_i) E\{\nu_i(x_i, v_i)/Z_i\} . \quad (58)$$

Given z_i, the random variables x_i and v_i are no longer independent. Therefore,

$$E\{\nu(x_i, v_i)/Z_i\} \neq 0 \quad (59)$$

and forms one source for which the estimates are seen to be biased since this bias term adds into the error propagation equation (58).

The process noise forms an additional source of bias in the estimates. The error from one stage to the next is

$$\bar{e}_{i+1} = A_i e_i + w_{i+1} \quad (60)$$

where w_i is a vector of white process noise. Taking the expectations of Equation (60) conditioned on Z_i and introducing this into Equation (58) gives

$$E\{e_i/Z_i\} = L_i(z_i) A_{i-1} E\{e_{i-1}/Z_i\} - K_i(z_i) E\{\nu_i/Z_i\} + E\{w_i/Z_i\} . \quad (61)$$

Similarly,

$$E\{e_{i-1}/Z_i\} = L_{i-1}(z_{i-1})A_{i-2} E\{e_{i-2}/Z_i\} - K_{i-1}(z_{i-1}) E\{\nu_{i-1}/Z_i\} + E\{w_{i-1}/Z_i\} , \quad (62)$$

that is, a recursion rule results in going from stage to stage where the conditioning on the measurement history remains fixed. The solution of this recursion is of the form

$$E\{e_i/Z_i\} = \underline{\Phi}_{i,0}\, E\{e_0/Z_i\} + \sum_{j=0}^{i-1} \underline{\Phi}_{i,j+1}\, [E\{w_j/Z_i\} - K_j(z_i)\, E\{\nu_j/Z_i\}] \tag{63}$$

where

$$\underline{\Phi} = \prod_{k=j}^{i} L_k\,(z_k)\, A_k\ . \tag{64}$$

If the gain $K_i(z_i)$ is chosen as derived for the deserver of subsection IIB, then as i goes to infinity, $\underline{\Phi}_{i,0}$ goes to zero. Since the filter has this inherent stability, the magnitude of the steady-state error as i tends to infinity will depend upon the speed of convergence of $\underline{\Phi}_{i,0}$. Note that process noise and measurement noise both contribute to the biasing.

There may well be better choices for the gains used in the filter which will reduce the bias in the estimates. A somewhat similar conceptual problem is that of estimating the parameters of a constant coefficient linear system with noise observations. Instrumental variables has been suggested as an approach.[4] This approach, implemented without process noise, has been used[2] for the pseudolinear filter with some success.

4. K. Y. Wong and E. Polak, "Identification of Linear Discrete Time Systems Using the Instrumental Variable Method," *IEEE Transactions on Automatic Control*, Vol. AC-12, No. 6, December 1967.

III. THE ADAPTIVE EXTEND KALMAN FILTER AND AN ADAPTIVE HOMING GUIDANCE LAW BASED ON THE EXPONENTIAL COST CRITERION

The previous section describes the observability of the states of the homing engagement using angle-only information. Furthermore, difficulties and directions for constructing a filter using pseudolinear measurements have been discussed. In this section the established extended Kalman filter (EKF) in rectangular coordinates is used to process the noisy angle information. This filter is used in cascade with an optimal guidance law previously derived from linear quadratic Gaussian (LQG) theory. Two new features are considered to enhance the system performance. First, the measurement noise (and process noise) variance is estimated on-line using a sliding window estimation procedure.[5] The inclusion of this procedure is not very numerically costly since the error variance had to be calculated on-line for the EKF. In a sense, the EKF is adaptive to the missile engagement. By estimating the measurement noise variance on-line, the EKF is adaptive with respect to the noise environment. Since the error variance is already calculated on-line, an adaptive guidance law based on the exponential cost criterion can be mechanized without a great deal of numerical cost in hopes of further reducing miss distance, especially against highly maneuverable targets. This scheme is tested on a six-degree-of-freedom simulation in which a bank-to-turn missile is modeled.

In subsection IIIA the six-degree-of-freedom simulation is described. In subsection IIIB the EKF formulation is discussed. The adaptive scheme for determining measurement and process noise variance on-line is given in subsection IIIC. Numerical results on estimating the measurement variance on-line are also presented. The adaptive guidance law based upon the linear-exponential-Gaussian (LEG) theory[6] is presented in a form used in its implementation as a homing missile guidance law in subsection IIID. Numerical results showing the performance of the LEG adaptive guidance relative to the LQG guidance when both use estimates from the adaptive EKF are also given in subsection IIID.

A. Six-Degree-of-Freedom Simulation

The six-degree-of-freedom model of a bank-to-turn missile is in modular form, allowing easy modification of one element without altering the remaining elements. The elements

5. J. Simmons; S. Balakrishnan; J. Speyer; and D. Hull, [illegible] Comparison of Optimal Filters, Report AFATL-TR-79-87, Air Force Armament Laboratory, Air Force Systems Command, Eglin Air Force Base, Florida, October 1979.

6. J. L. Speyer, "An Adaptive Terminal Guidance Scheme Based on an Exponential Cost Criterion with Application to Homing Missile Guidance," *IEEE Transactions on Automatic Control*, Vol. AC-21, No. 3, June 1976.

are the missile airframe aerodynamics, the seeker, the guidance/estimation algorithm, and the autopilot. Since the engagement is normally restricted to altitudes below 82,000 ft, only the troposphere and stratosphere are modeled. The autopilot model for this bank-to-turn missile processes yaw-and-pitch rate acceleration commands from the guidance law, and accelerometer and rate gyro information to produce missile control surface deflections. The autopilot model is divided into four distinct elements: yaw, pitch, and roll channels and a self-adaptive network. The integration subroutine uses a fixed-step, fourth-order, Runge-Kutta method to integrate the system differential equations. Subroutines are available for one- and two-dimensional linear interpolation of the aerodynamic coefficients, which are functions of Mach number and angle-of-attack or sideslip angle.

The target is modeled as a point mass. It maintains a constant speed throughout the engagement. From the time of launch to a relative range of 6000 ft, the target flies steady and level at the launch altitude. Once this activation range is reached, the target initiates a 45-deg maneuver up and to the right relative to its reference frame at maximum g. This maneuver is maintained until the time-to-go reaches 1 sec when the target instantaneously rolls 180 deg and pulls maximum g for the remainder of the engagement.

B. The Extended Kalman Filter

Studies[5] involving various forms of the EKF both in rectangular and spherical coordinates have indicated that the EKF in rectangular coordinates is quite robust. The dynamic system in rectangular coordinates used on the filter is given by Equation (1) where the coefficients are presented in Equations (29) and (30). The assumption here is that the target sensor is the main error source and that missile sensors are perfect. Therefore, u_i, the missile acceleration measured by accelerometers, is known with negligible error. The major modeling assumption is that the target can be modeled as a Gauss-Markov process in the filter. The essential idea is that the autocorrelation function of this Gauss-Markov model is the same as that obtained from a Poisson process, which more accurately models the target maneuver. The actual target is assumed highly maneuverable and a preprogrammed target maneuver is used on all simulation runs as described in subsection IIIA.

The measurements are assumed to be of the form given in Equation (51), which are noisy observations relative to an inertial reference frame. This is necessary to estimate relative attitude and target motion. The assumption is that the tracking and stabilization algorithms isolate the target sensor from the missile body. In a skid-to-turn missile, a two-axis gimbal system with a roll-stabilized coordinate frame usually is sufficient to preserve the inertial reference. In the bank-

to-turn missile, additional compensation must be used because of the high roll rates employed by the autopilot.

In all the simulations that have been performed, only angle information is used. Observered boresight angle errors and seeker pitch-and-yaw rates are assumed to lie in a roll-stabilized inertial coordinate system. Then, the inertial angles measurements are simply integrated pitch-and-yaw rates added to their respective boresight angle errors obtained from the centroid of the blur circle on the IR screen. The essential noise source has been assumed to reside with the measurement of the boresight angle errors. Although the noise is assumed to be white with zero mean, the siding window adaptive scheme estimates both the measurement noise variance and biases. These biases may be attributed in part to nonlinear effects in the EKF.

The EKF applied to the homing engagement is based upon a linearization of the observations which are nonlinear in the rectangular reference frame. Because of the linearity of the dynamic system Equation (1), from the last state estimate, $\hat{x}_{K/K}$, closed-form formulas for the predicted state estimate $\hat{x}_{K+1/K}$, and the error covariance, $P_{K+1/K}$, are obtained [Equations (29) and (30)]. The subscript K+1/K means that the state is at time t_{K+1}, but the last observation update occurred at t_K. The state estimate update equations for processing and observation are obtained by linearizing the measurement function about the extrapolated estimate $\hat{x}_{K+1/K}$. The update equation for the state utilizes the nonlinear observation equations, while the update equation for the error variance uses the equations that are obtained from a perturbed linear filter formulation about $\hat{x}_{K+1/K}$. Since $\hat{x}_{K+1/K}$ is not known a priori, the error variance must be propagated on-line, and, thereby, the filter gains are calculated on-line. Note that in constructing the gains for the pseudomeasurement observer, no linearization is necessary, although P_i must be calculated on-line since $H_i(z_i)$ is not known a priori.

C. On-Line Estimation of the Measurement and Process Noise Variances

In practice, the actual noise and process noise variances are not known since various targets have different noise signatures. In the case of the IR sensor, which is operational a relatively long time, estimation of the observation and the state process noise variances can be accomplished on-line.

The approach used is that given in Reference 5 where the population means and covariances are determined by using the predicted observation residuals sampled and stored over a sequence of m past estimates. The finile memory filter assumption is used to retain a population of m observation residuals

which is used sequentially to determine a current value of the observation and process noise covariances.

The algorithm for estimating the measurement noise statistics is given here. The algorithm for estimating the process noise statistics is given in Reference 5 and is similar to the scheme now presented. Emphasis in numerical experiments has been placed largely on the estimation of measurement noise statistics. The measurement function [Equation (2)] with additive Gaussian white noise is

$$z_i = h_i(x_i) + v_i \ . \tag{65}$$

The objective is to estimate the mean and variance of v_i from the measurement residuals r_i obtained from the EKF as

$$r_i = z_i - h_i(\hat{x}_{i/i-1}) \ . \tag{66}$$

The residuals represent the error in the actual and predicted observations and are used as a measure of the measurement noise mean and variance. In the limit that the EKF approaches a conditional mean estimator, the measurement residuals are a zero mean white noise process with variance

$$E[r_i \ r_i^T] = R_i + h_x(\hat{x}_{i/i-1}) \ P_{i/i-1} \ h_x^T \ (\hat{x}_{i/i-1}) \ , \tag{67}$$

where R_i is the measurement variance and $h_x(\hat{x}_{i/i-1})$ is the partial derivative of h_i with respect to its argument evaluated at $\hat{x}_{i/i-1}$.

By using statistical sample theory, the mean and variance of the residuals are determined and are then related to the sampled mean $\bar{v}_i$ and variance $\bar{R}_i$ of the measurement noise through Equation (67). Suppose the sample window has N samples of the residuals; then the sample mean can be written in the recursion form,

$$\bar{v}_i = \frac{1}{N} \sum_{k=i-N+1}^{i} \bar{v}_k = \bar{v}_{i-1} + \frac{1}{N} [r_i - r_{i-N}] \ . \tag{68}$$

In order to mechanize this scheme, N samples must be stored. In a similar way, the sample variance of the residuals is used with Equation (67) to form the same measurement variance as

$$\bar{R}_i = \frac{1}{N-1} \sum_{k=i-N+1}^{i} \{ (r_k - \bar{v}_k)(r_k - \bar{v}_k)^T - \frac{N-1}{N} \ h_x(x_{k/k-1}) P_{i/i-1} \ h_x^T(\hat{x}_{k/k-1}) \} \tag{69}$$

where a recursion relation can be formed as

$$\bar{R}_i = \bar{R}_{i-1} + \frac{1}{N-1}\{(r_i - \bar{v}_i)(r_i - \bar{v}_i)^T$$
$$- (r_{i-N} - \bar{v}_{i-N})(r_{i-N} - \bar{v}_{i-N})^T$$
$$+ \frac{1}{N}(r_i - r_{i-N})(r_i - r_{i-N})^T$$
$$- \frac{N-1}{N}[h_x(\hat{x}_{i/i-1})P_{i/i-1}\, h_x^T(\hat{x}_{i/i-1})$$
$$- h_x(\hat{x}_{i-N/i-N-1})\, P_{i-1/i-N-1}\, h_x^T(\hat{x}_{i-N/i-N-1})]\}. \qquad (70)$$

The division by N-1 rather than N is due to the requirement that sample variance be unbiased. The sample mean and variance recursions are begun with a batch average over the N samples where Equation (69) is used for the sample variance but $\bar{v}_k$ is fixed at $\bar{v}_N$.

Initializing the variance recursion by a batch process produces a bias in the variance estimate since the residuals are constructed by the filter using the stored a priori measurement noise variance. If the actual measurement noise variance, R_A, is larger than the a priori variance, R, assumed in the filter, then the sum of the residuals in Equation (69) will dominate the term $h_x\, P_{i/i-1}\, h_x^T$. This is because the residuals should be larger than if R_A is used, and the error variance $P_{i/i-1}$ calculated using R is smaller than it would be if R_A were used. Therefore, the estimated $\bar{R}_i$ should be larger than R_A. This is conjectured to be a conservative approach since by obtaining an $\bar{R}_i > R_A$, the filter will not heavily weigh the current data. If $R_A < R$, then the sum of the residuals in Equation (69) will be dominated by $h_x\, P_{i/i-1}\, h_x^T$. In fact, $\bar{R}_i$ can be made zero. Therefore, if $\bar{R}_i < R_A$, then Equation (70) is initialized by the estimated variance of the residues, i.e., the second term is neglected. Therefore, $\bar{R}_N$ will be greater than R_A. However, it will be much less than R.

Careful checking of the computer code for this algorithm showed that a numerical error existed in the previous code[5]. This error has been corrected, and experimentation has begun on the six-degree-of-freedom simulation. The launch scenario is defined by the following data: altitude = 10,000 ft; Mach number = 0.9; launch range = 3,000 ft; boresight angle = 0 deg and aspect angle = 60 deg.

The actual measurement variance used to produce the noise sequence corrupting the measurement to the EKF is

$$\sigma^2 = M\sigma^2/\Delta T \ , \ \sigma = \text{as, el}$$

where σ^2 is a power spectral density characterized as a function of relative range as

$$\sigma_{\theta}^2 = \sigma_{-1,\theta}^2 / R^2 = \sigma_{g\theta}^2, \quad \theta = az, el.$$

In the simulation

$$\sigma_{-1,\theta} = 0.25 \text{ rad}^2 \text{ ft}^2 \text{ sec}, \quad \sigma_{0,\theta}$$

$$= 56.25 \times 10^{-8} \text{ rad}^2 \text{ sec}; \quad \theta = az, el .$$

Also, ΔT is the sample time, which is 0.02 sec and M is the mismatch parameter, being the ratio of the actual noise variance to that used in initializing the filter for the adaptive scheme or that used by the EKF when the adaptive feature is not present.

The following experimentation was begun to test the effect of the adaptive feature and to determine the size of the sliding window, N. Table 1 represents results from single-shot realizations. The results of this study are preliminary since a Monte Carlo analysis using at least 10 runs would be more represenative. If M = 50, the adaptive feature seems to produce significant improvements in miss performance. These preliminary results seem to indicate that miss distance depends heavily on measurement variance. It might be argued that the guidance system reduces the miss variance to a minimal value which is that of the variance of the error in estimating the miss by the filter. Therefore, improvements in the filter estimates will be reflected in miss distance.

The tracking histories of the estimated value of the measurement variance against the actual error variance are given in Figures 11 through 18. Both the variances associated with elevation and azimuth are given for M = 50 and M = 0.02 where N - 20. Two sets of figures are given for each M to effect scale. During the first 0.4 sec, the filter uses the stored measurement variance with M = 1. After N = 20 samples have been accumulated, the estimated measurement variance is used in the EKF. In Figures 11 and 12, the tracking history of the measurement variance is displayed in an expanded scale. The estimates are on the order of magnitude of that of the actual value. Near terminal the actual error variance rises quickly. The estimates tend to lag the actual value. This is best seen in Figures 13 and 14. This is not surprising in that the estimator assumes a constant rather than a variable measurement variance. Also, near terminal the error variance of the state estimate tends to decrease. This means that the last two terms of Equation (70) tend to be negative. This effect is more pronounced when M = 0.02. In fact, the constant values near terminal shown in Figures 15 and 16 are caused by a fix in the program that chooses the last value of the estimate before it goes negative. The sharp changes in the estimate of the measurement variances are seen in Figures 17 and 18. Note that in Figures 15 and 16, using the expanded scale, the estimated variances are larger on the average than the actual variances. This behavior has not been explained although it is conservative.

TABLE 1. MISS DISTANCE VS. SLIDING WINDOW SAMPLE SIZE FOR M = 50 AND M = 0.02 USING A SINGLE REALIZATION

Mismatch (M) = 50		Miss Distance (ft)
Extended Kalman Adaptive R	N = 0	91.529
	N = 20	25.260
	N = 30	59.464
	N = 40	56.837
	N = 50	39.584
		426.612
Mismatch (M) = 0.02		**Miss Distance (ft)**
Extended Kalman Adaptive R	N = 10	32.268
	N = 20	27.182
	N = 30	28.662
	N = 40	70.158
	N = 50	57.594
		10.835

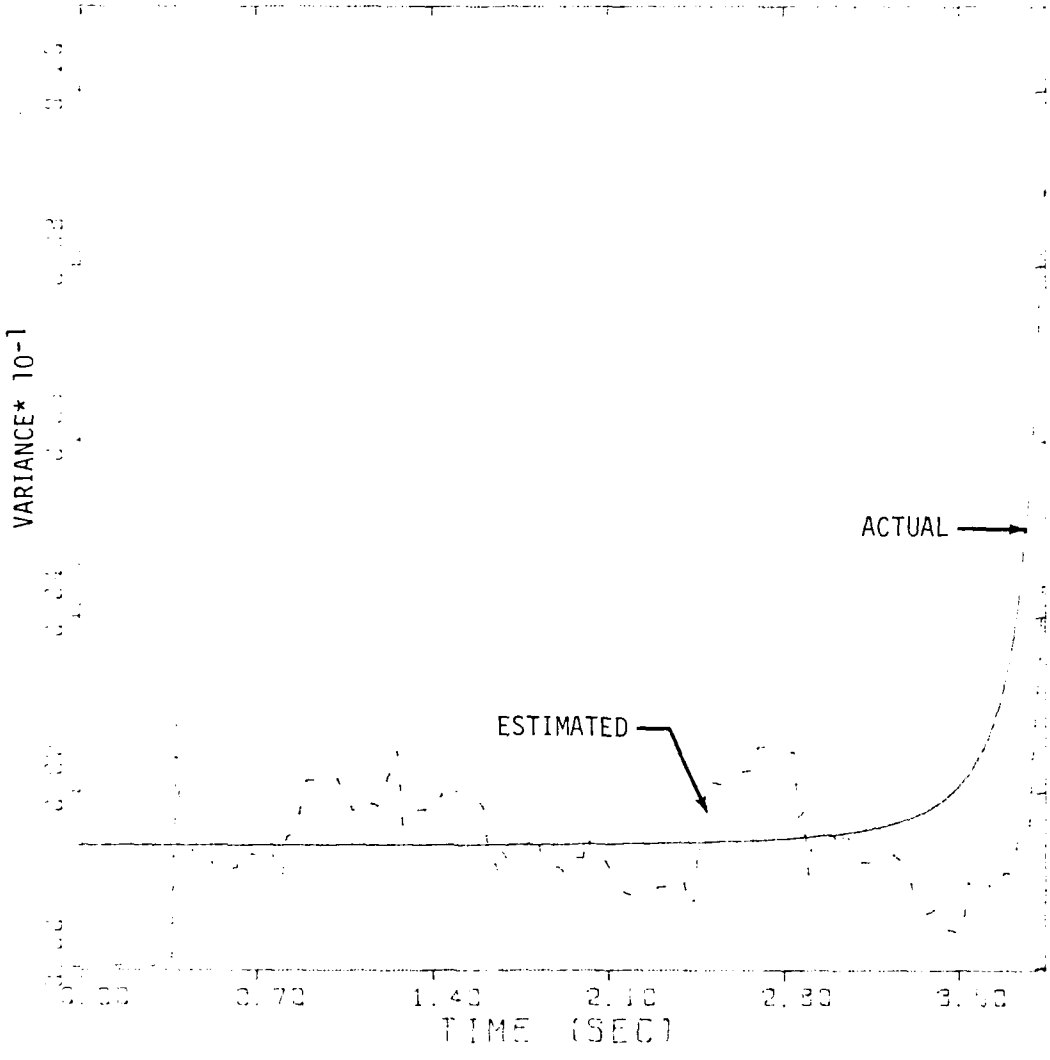

Figure 11. Azimuth measurement variance estimate for M = 50 and N = 20 in expanded scale.

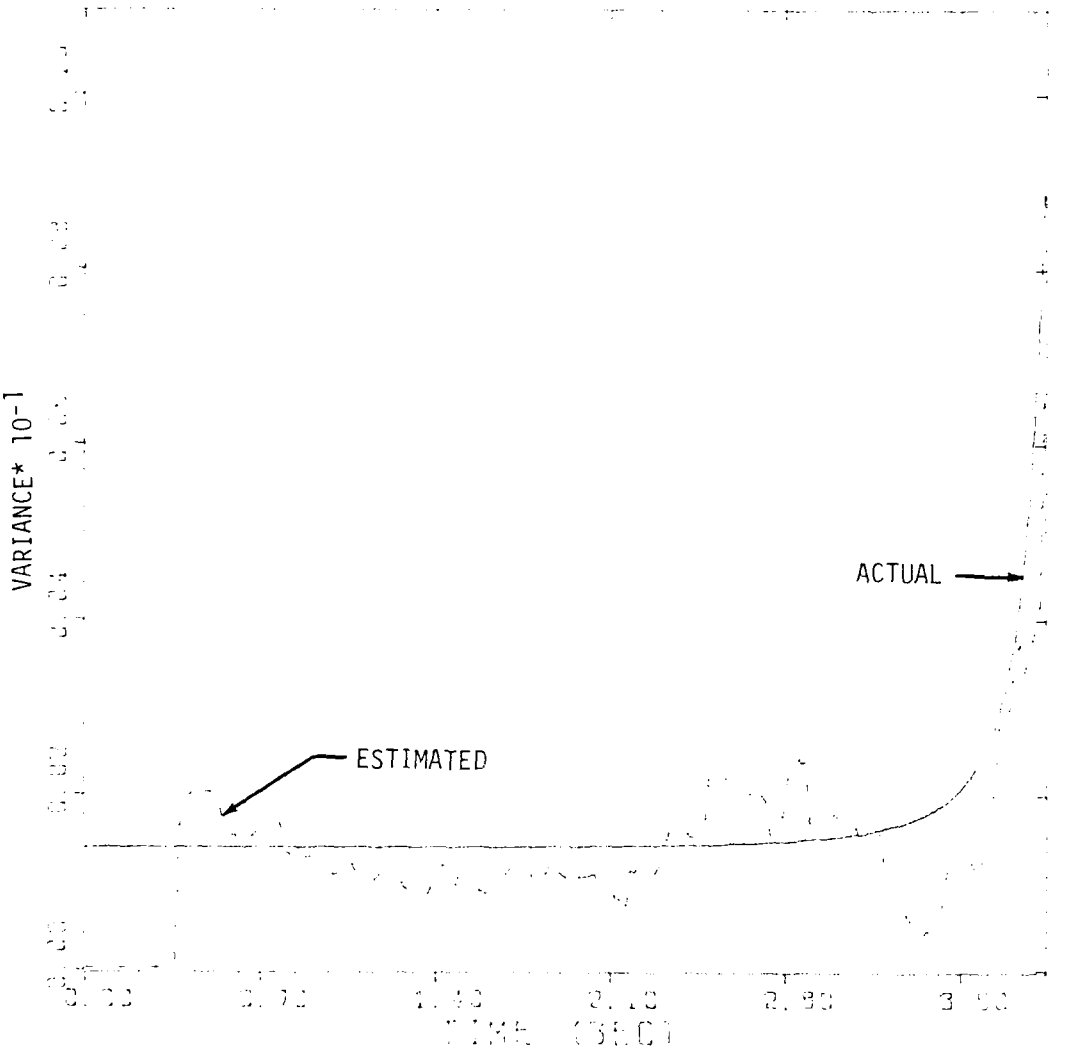

Figure 12. Elevation measurement variance estimate for M = 50 and N = 20 in expanded scale.

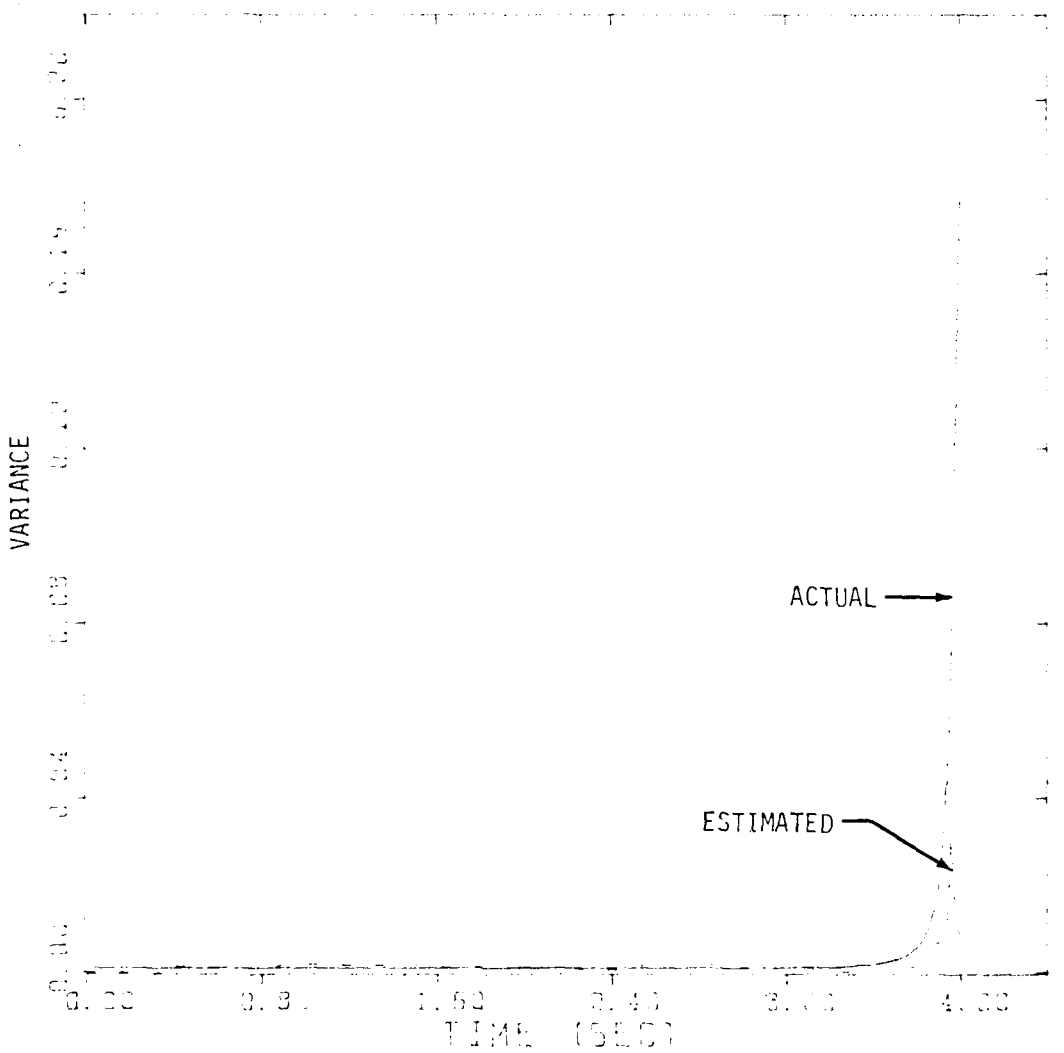

Figure 13. Azimuth measurement variance estimate for M = 50 and N = 20.

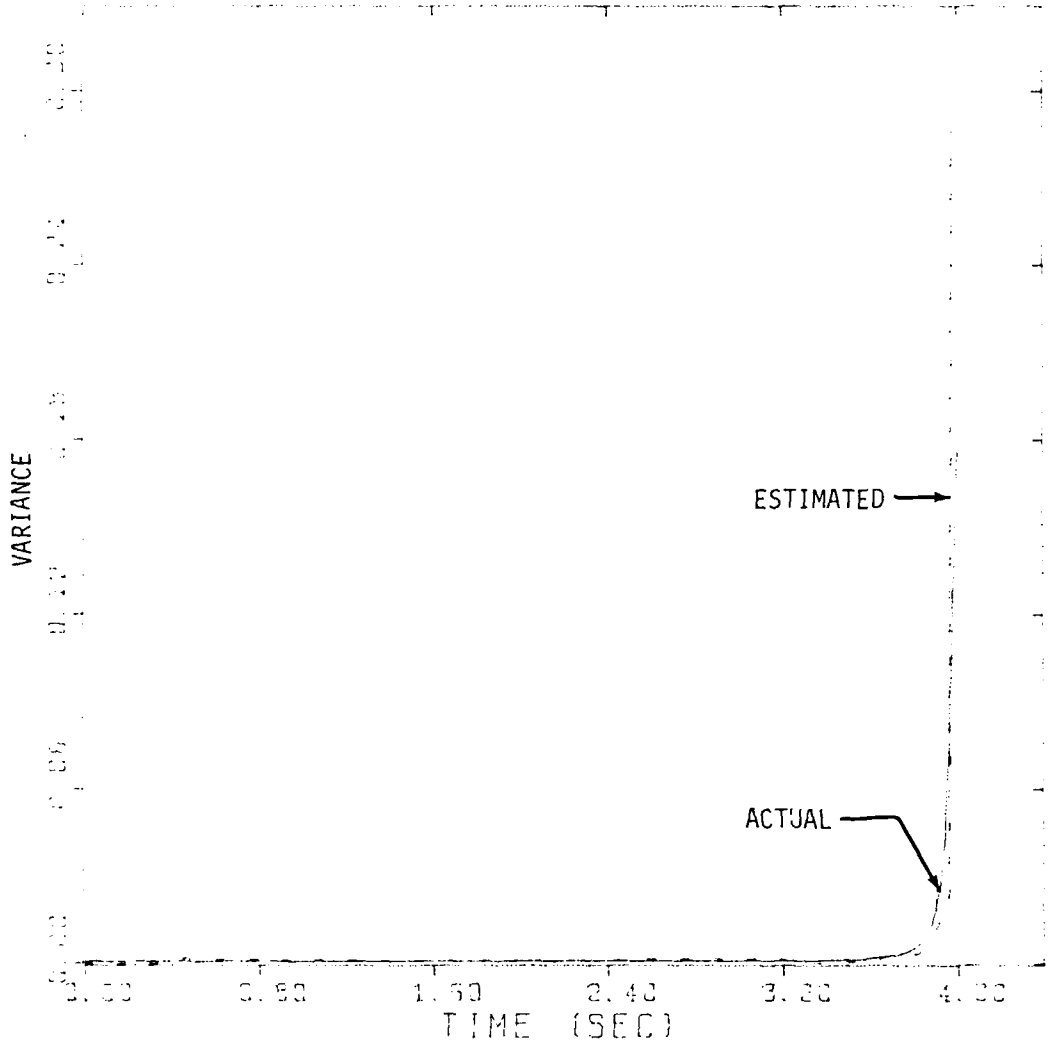

Figure 14. Elevation measurement variance estimate for M = 50 and N = 20.

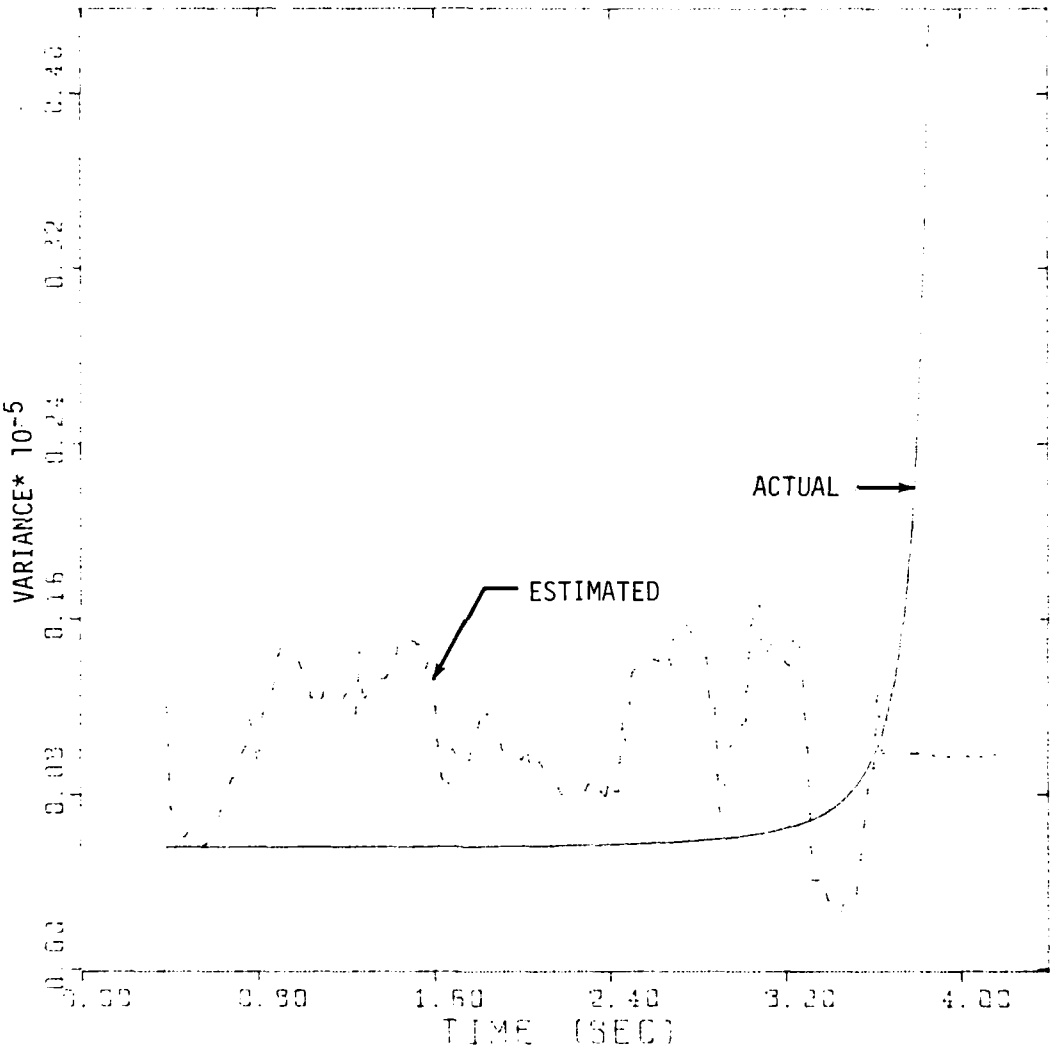

Figure 15. Azimuth measurement variance estimate for M = 0.02 and N = 20 in expanded scale.

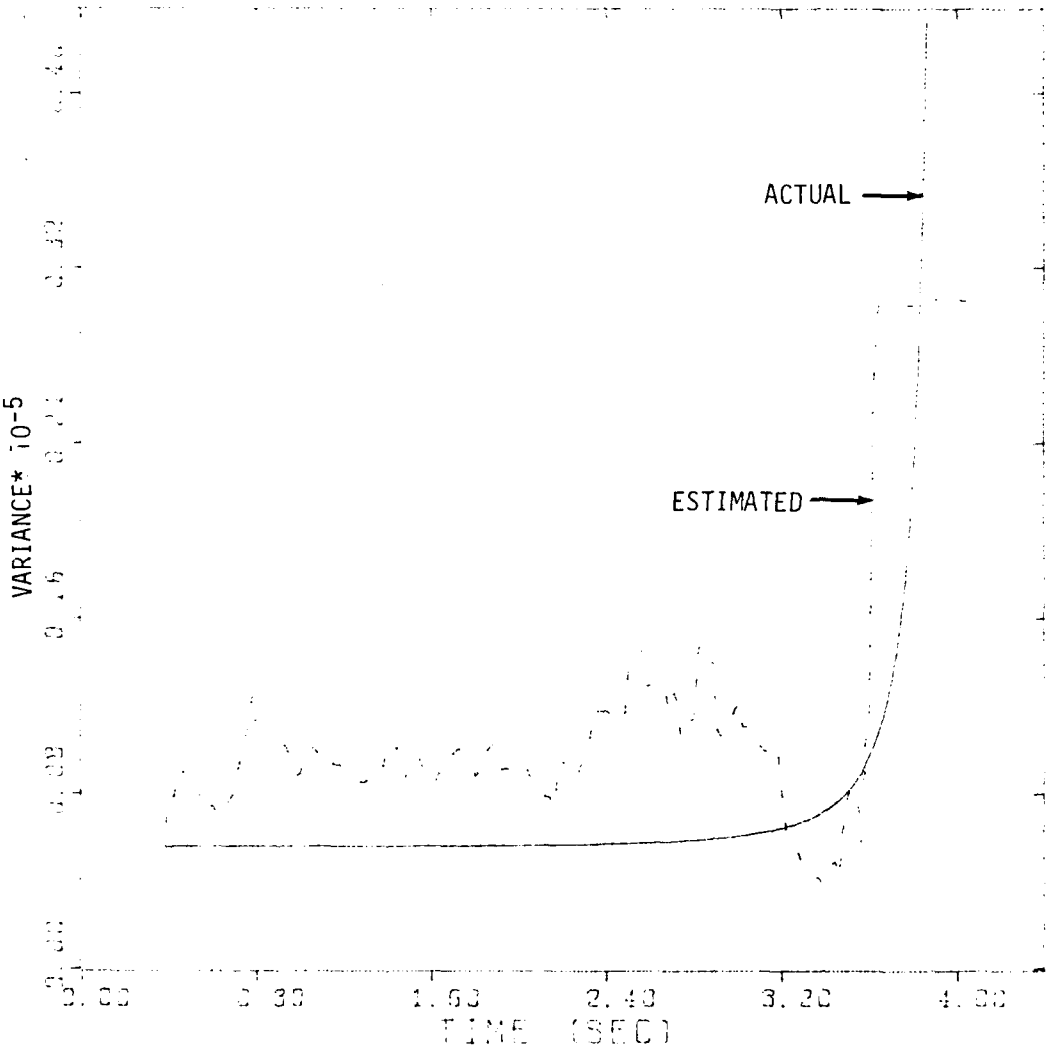

Figure 16. Elevation measurement variance estimate for M = 0.02 and N = 20 in expanded scale.

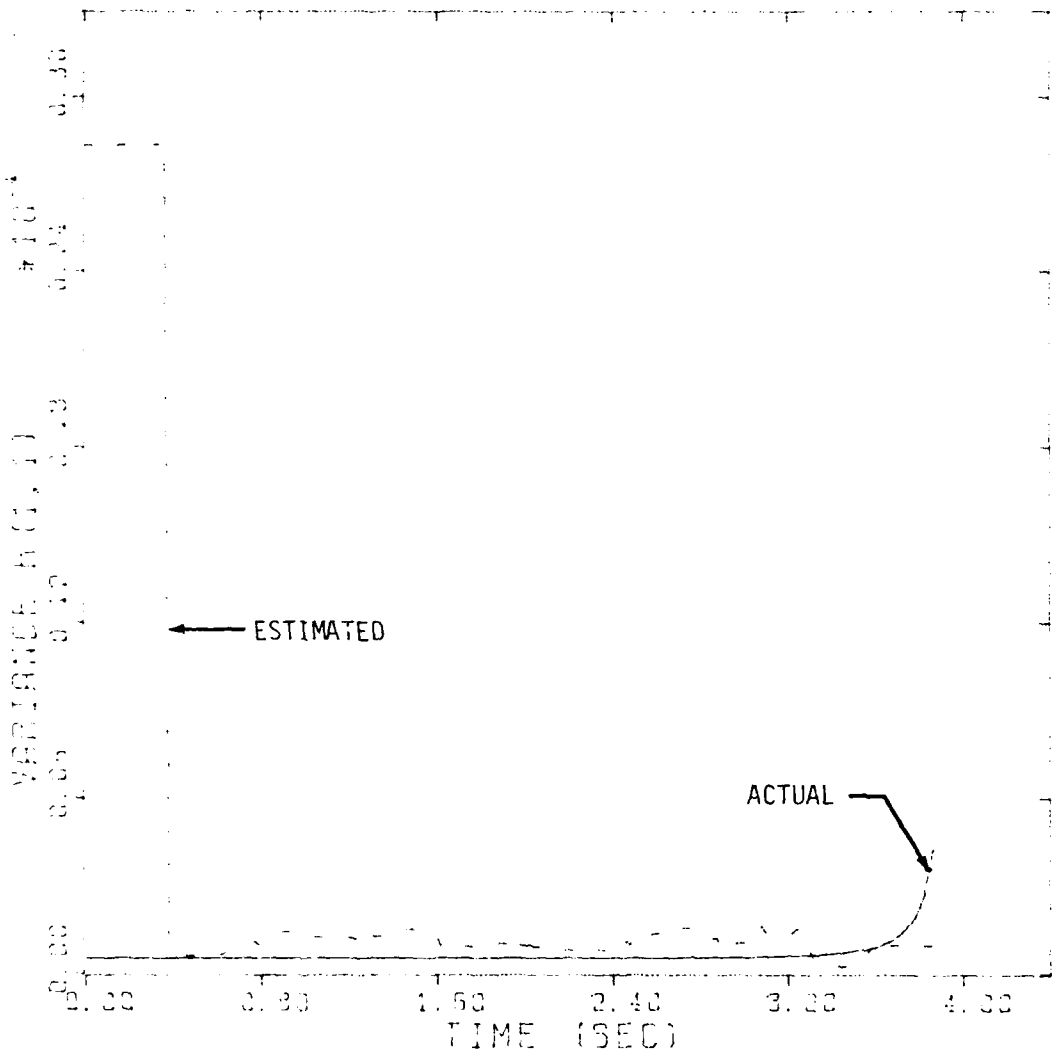

Figure 17. Azimuth measurement variance estimate for M = 0.02 and N = 2.

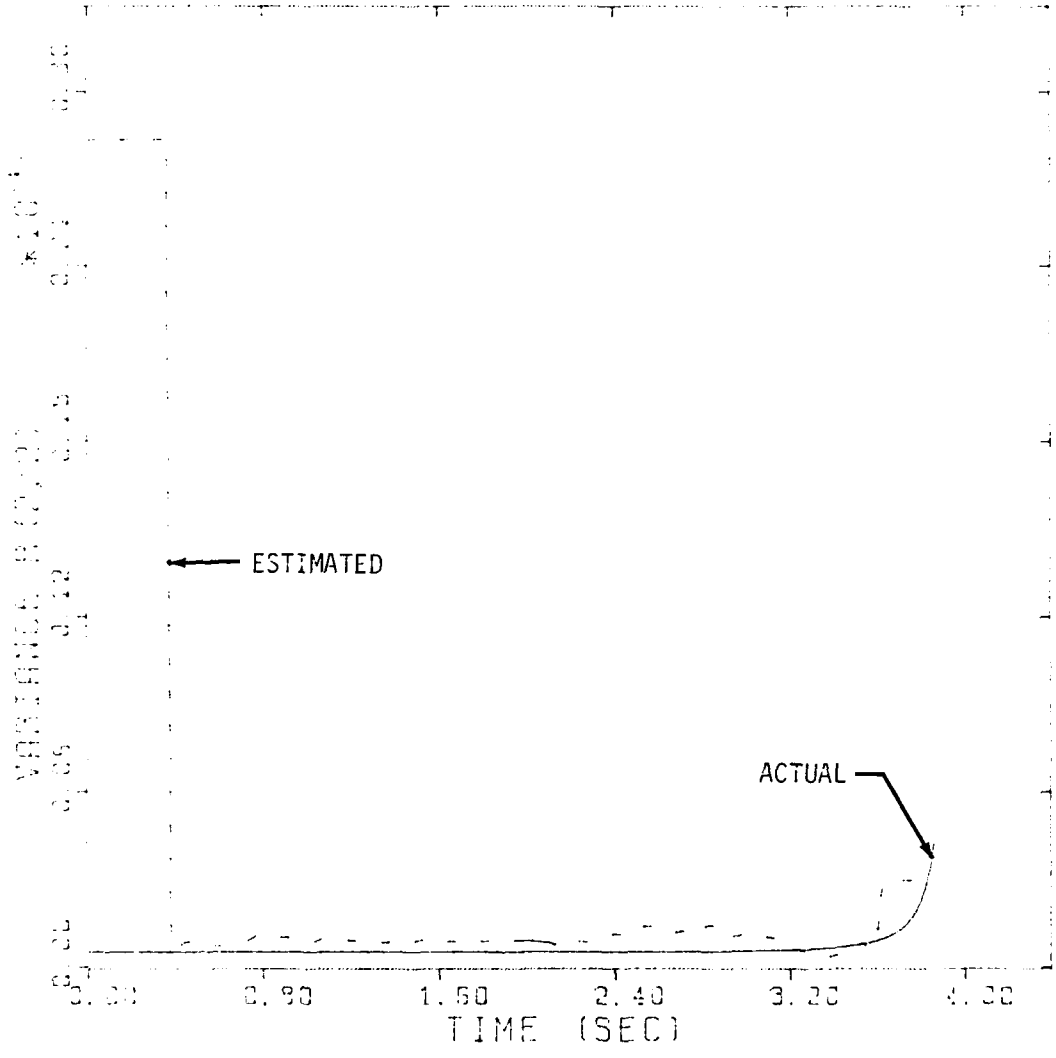

Figure 18. Elevation measurement variance estimate for M = 0.02 and N = 20.

D. Adaptive Homing Guidance Scheme Based Upon LEG Theory

The LEG theory[5] is a generalization of the LQG theory. Therefore, the LQG guidance rule used in subsection IIF is modified; the extent of the modification is not very large. The LEG problem is that a control law for u(1) is to be determined which minimizes the exponential cost criterion

$$J = E\{\mu \exp \mu \psi\} \tag{71}$$

where ($Q_f > 0$ and $\underline{R} > 0$),

$$\psi = x(t_f)^T Q_f x(t_f) + \int_0^{t_f} u^T R u \, dt, \tag{72}$$

subject to the dynamic equation

$$\dot{x} = Fx + Gu + w \tag{73}$$

and the measurement process

$$z = Hx + v \tag{74}$$

where the n-dimensional, normally distributed initial state x_0 and the n-and q-dimensional Gaussian white noise processes w and v are assumed to be zero mean with variances

$$E[x_0 \; x_0^T] = P_0$$

$$E\{w(t) \; w(\tau)^T\} = W\delta(t - \tau)$$

$$E\{v(t) \; v(\tau)^T\} = V\delta(t - \tau) \; . \tag{75}$$

Note that the cost criterion is an exponential of a graduated form. The control law determined from LEG theory reduces to that of the LQG theory as the parameter μ approaches zero. If $\mu > 0$, then large excursions in state and control are heavily penalized, whereas if $\mu < 0$, a less active control rule results.

The resulting control rule is linear in the estimated state $\hat{x}$ as

$$u = -\underline{R}^{-1} G^T Q \hat{x} \tag{76}$$

where

$$Q = (I - \mu SP)^{-1} S \tag{77}$$

where P is the error covariance matrix produced in the filter and S satisfies a matrix Riccati equation of the form

$$-\dot{S} = SF + F^T S - S(GR^{-1} G^T - \mu W)S_j \quad S(t_f) = Q_f \ . \tag{78}$$

In applying this controller to the homing guidance problem, u is the missile acceleration command, F and G are given by Equation (28) and w is the white noise forcing term in the Gauss-Markov target model

$$w^T = [0, \ 0, \ I_3 \ w_T] \tag{79}$$

with power spectral density

$$W = \begin{bmatrix} 0 & 0 & 0 \\ 0 & 0 & 0 \\ 0 & 0 & I_3 \ W_T \end{bmatrix} \ . \tag{80}$$

In the cost function

$$\underline{R} = \gamma I_3 \ , \quad Q_f = \begin{bmatrix} \Theta I_3 & 0 & 0 \\ 0 & 0 & 0 \\ 0 & 0 & 0 \end{bmatrix} \ . \tag{81}$$

The solution to the matrix Riccati equation (78) is

$$S(\tau_g) = \frac{\Theta I_3}{K_1+K_2} [I_3, \ I_3 \ \tau_g, \ I_3 \ f_T]^T \ [I_3, \ I_3 \ \tau_g, \ I_3 \ f_T] \tag{82}$$

where $\tau_g \triangleq t_f - t$, the time-to-go, and

$$f_T = [e^{-2v\tau_g} + 2v\tau_{g-1}]/4v^2 \tag{83}$$

$$K_1 = 1 + \frac{\Theta}{\gamma} \frac{\tau_g^3}{3} \tag{84}$$

$$K_2 = -\mu w_T \Theta \left\{ \frac{\tau_g^3}{3(2v)^2} - \frac{1}{2(2v)^5} \left(e^{-2v\tau_g} - 1 + 2v\tau_g e^{-2v\tau_g} \right) \right.$$
$$+ \frac{1}{(2v)^5} \left[-(2v)^2 \ \tau_g^2 + 2v\tau_g - 2v\tau_g \ e^{-2v\tau_g} \right]$$
$$\left. - \frac{1}{2(2v)^3} e^{-2v\tau_g} \ f_T \right\} \ . \tag{85}$$

In Reference 6, the sign of the coefficient of the first term of Equation (85) was incorrect. If $\mu = 0$, then the controller reduces to that of the LQG controller. For $\mu \neq 0$, $S(\tau_g)$ changes by the addition of K_2. This controller is adaptive because of the presence of the error variance in Equation (77).

In Reference 6, the positive exponential cost criterion was used. The result was that the tails of the miss distribution were reduced. This may be partially explained by noting that the guidance scheme would be less sensitive to large target maneuvers. The positive exponential solution for the perfect measurement problem is the same as that obtained from the differential game problem where the process noise is considered a control variable and the weighting in the cost function is that of the inverse of the power spectral density $W_T I_3$. The numerical experimentation with this controller has been with the positive exponential. One difficulty to be avoided is that μ must be set small enough such that $I - \mu PS > 0$. The values of ϑ, γ, μ, and w_T are chosen so that the navigation ratio increases from 3 of the LQG guidance scheme. Figure 19 shows the navigation ratio vs. time-to-go for various values of the parameter. The ragged behavior near terminal shows the effect of the error variance on the navigation ratio. Its effect shows up here mostly due to $S(\tau_g)$ becoming large rather than P becoming large. The best miss distance was obtained by the LQG controller, although the difference from that obtained by the LEG guidance law is quite small. It must be emphasized that the results presented here are for only one realization on which the LEG guidance law was tuned. A Monte Carlo analysis should be performed so that the major advantage of the LEG guidance rule in pulling in the tails of the miss distribution can be assessed.

IV. CONCLUSIONS

The pseudolinear measurement observer provides important insight into the behavior of angle-only measurement homing engagements. Clearly, from the numerical results the system is observable. This study showed the effect of changes in the parameters of the filter on the observer performance. By analogy with the Kalman filter, these parameters are related to initial error variance, measurement noise variance, and process noise variance. In the context of this controlled experiment, filter sensitivity can be assessed. As the measurement noise variance increases, the response time of the observer decreases. The observer seems quite insensitive to variations in the initial error variance for the target motion. However, the response of the observer is quite sensitive to the process noise parameter. The effect here is important and deserves further study.

The extension of the pseudolinear measurement observer to a stochastic filter has the difficulty of producing biased estimates. However, since all measurements used with either IR or radar sensors can be put into the pseudolinear form with additive state-dependent noise and since the filter requires no linearization, it is important to investigate filter structures which allow reduction of these biases.

The adaptive EKF in cascade with an adaptive guidance law based upon LEG theory has been investigated. A sliding window

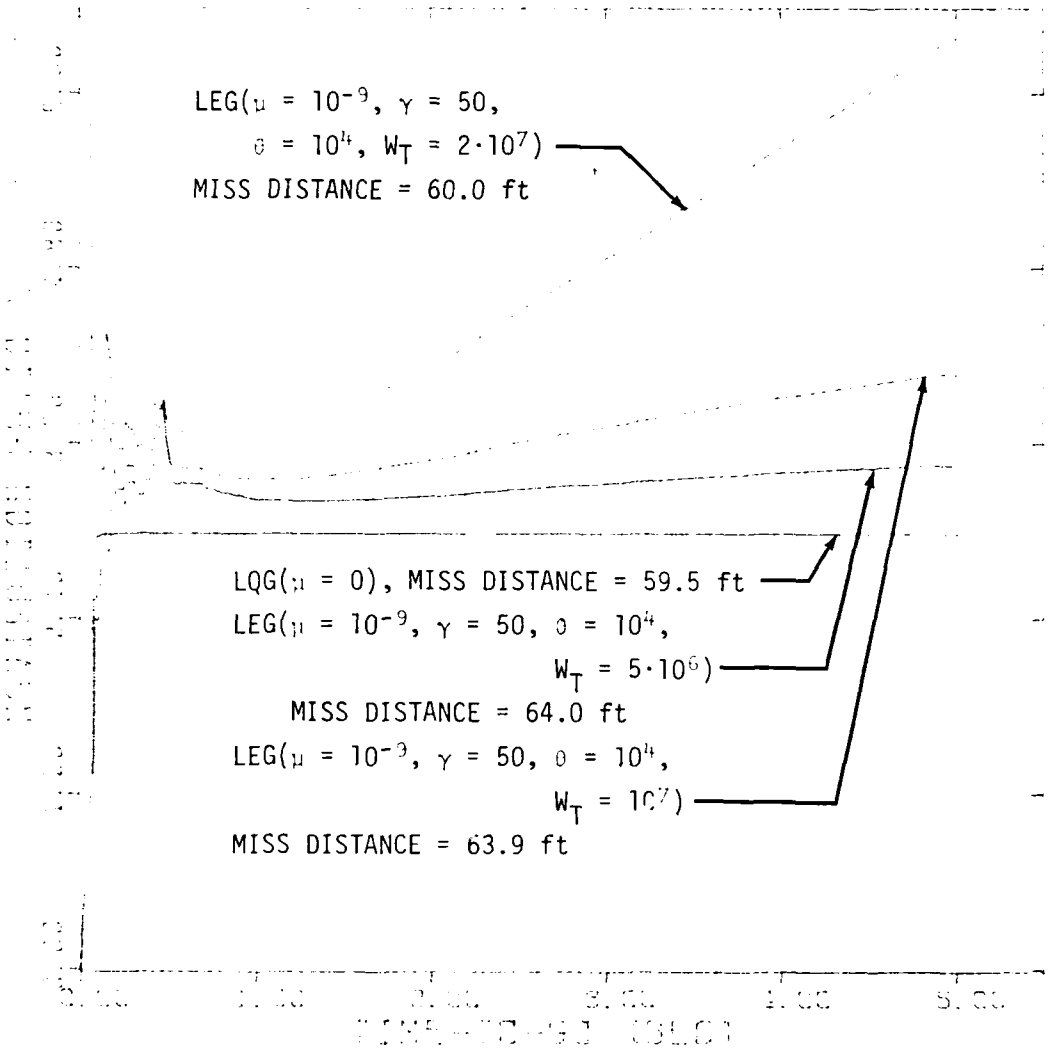

Figure 19. Navigation ratio for LQG and LEG guidance in the X-channel.

estimator has been used to process the residuals of the EKF so that the measurement noise variance could be determined on-line. This is a driver of the error variance in the EKF which is calculated on-line. The error variance is an input to the guidance law based upon LEG theory and is thereby adaptive. Estimating the measurement error variance on-line rather than using an priori measurement variance has important improvement in miss distance from our initial investigations. The adaptive feature of the guidance law should help reduce the tails of the miss distance distribution. Since only one realization of a missile engagement has been investigated, no significant miss distance results can be reported. However, the initial tuning of the LEG guidance law was performed using this realization. Monte Carlo studies on this LEG guidance law should be done to determine the capability of the system over an ensemble. With this study, the effect of the guidance system on the tails of the miss distance distribution can be assessed.

REFERENCES

1. Aidala, V. J., "Behavior of the Kalman Filter Applied to Bearings-Only Target Motion Analysis," *Advances in Passive Tracking*, Vol. I, NPS-62TS 77001, Naval Postgraduate School, May 1977.

2. Lindgren, A. G., and Gong, K. F., "Position and Velocity Estimation via Bearing Observations," *IEEE Transactions on Aerospace and Electronic Systems*, Vol. AES-14, No. 4, July 1978.

3. Bayson, A. E., and Ho, Y.-C., *Applied Optimal Control*, Blaisdell, Waltham, Massachusetts, 1969.

4. Wong, K. Y., and Polak, E., "Identification of Linear Discrete Time Systems Using the Instrumental Variable Method," *IEEE Transactions on Automatic Control*, Vol. AC-12, No. 6, December 1967.

5. Sammons, J.; Balakrishnan, S.; Speyer, J.; and Hull, D., *Development and Comparison of Optimal Filters*, Report AFATL-TR-79-87, Air Force Arnament Laboratory, Air Force Systems Command, Eglin Air Force Base, Florida, October 1979.

6. Speyer, J. L., "An Adaptive Terminal Guidance Scheme Based on an Exponential Cost Criterion with Application to Homing Missile Guidance," *IEEE Transactions on Automatic Control*, Vol. AC-21, No. 3, June 1976.

DISTRIBUTION

	No. of Copies
Defense Technical Information Center ATTN: DDC-TSR-1 Cameron Station - Building 5 Alexandria, Virginia 22314	2
DCASMA 908 South 20th Street Birmingham, Alabama 35205	1
US Army Materiel Systems Analysis Activity ATTN: DRXSY-MP Aberdeen Proving Ground, MD 21005	1
IIT Research Institute ATTN: GACIAC 10 West 35th Street Chicago, IL 60616	1
DRSMI-IYB, Mr. Smith	1
DRCPM - DT, Col. Williamson	1
DRSMI - R, Dr. McCorkle	1
- RG, Dr. Leonard	1
- RGN, Dr. Pastrick	1
- RGN, Mr. Murdock	2
- RPT, Record Set	1
- RPR	3
- LP, Mr. Voigt	1
Intergraph Corporation, Dr. Moyers	1
Dr. Speyer	1
Dr. Hull	1